Development of carbon ink for wearable sensors

A thesis submitted to the University of Manchester for the degree of

Master of Philosophy

In the School of Natural Sciences

Faculty of Science & Engineering

2020

Zihao Gu

Department of Materials

Table of contents

List of figures

List of tables

List of acronyms

NMP	N-methyl-2-pyrrolidone
IPA	Isopropyl alcohol
NPs	Nano-particles
PET	Polyester
CVD	Chemical vapour dispersion
AC	Activated carbon
CNTs	Carbon nanotubes
SWCNTs	Single-walled carbon nanotubes
MWCNTs	Multi-walled carbon nanotubes
GO	Graphene oxide
RGO	Reduced graphene oxide
h-BN	Hexagonal boron nitride
BP	Black phosphorus
CTP	Cone-to-plate
PTP	Plate-to-plate
SC	Sodium cholate
CMC	Critical micelle concentration
GLB	Hydrophile-Lipophile Balance Number
Na-CMC	Sodium carboxymethylcellulose
PVP	Polyvinylpyrrolidone
PS1	1- pyrenesulfonic acid sodium salt
SMS	Spun-bonded melt blown spun-bonded
PP	Polypropylene
CIJ	Continuous inkjet
DOD	Drop-on-demand inkjet
DSSCs	Dye-sensitised solar cells
PVAc	Polyvinyl acetate
PVA	Polyvinyl alcohol
PANI	Polyaniline
PVDF	Polyvinylidenefluoride
PCB	Printed circuit board

Abstract

Conductive inks play an important role in the production of smart textiles. Among them, water based inks have drawn high attention because water is environmental friendly, harmless and easy-dried solvent. In practice, coffee ring effect is one of the problems which exists in water-based inks and influences the uniformity of the coating/printing process. Meanwhile, particle size, viscosity and surface tension of the ink are other key factors which should be adapted based on the substrate fabric, impregnation method and final application.

This research aims at developing water-based carbon ink which is free from coffee ring effect for the construction of fine nonwoven polyester fabric based pressure sensors. Coffee ring effect leads to particles aggregation of functional particles among the edges of an ink drop during drying. Because of this, the functional particles are distributed non-uniformly on the substrate and lead to poor performance for the final application. This research works on the prevention of the coffee ring effect based on the Marangoni principle. During the research, ink was investigated with aspects to components, viscosity, surface tension and ink performance of the textile-based pressure sensor. In order to proof the elimination of coffee ring effect, scanning electron microscope (SEM) images were taken and analysed. The textile-based pressure sensors were constructed by applying inks on fine nonwoven polyester fabrics in order to evaluate performance of the ink. The sensors were produced with a sandwich structure and tested for capturing mechanical signals.

The research results showed the elimination of coffee ring effect on the substrate

textiles coated with the ink produced in this research. Textile-based nonwoven polyester pressure sensors produced in this research showed satisfactory properties. The sensors with carbon take-up rate of 70.6％ were able to achieve an average electronic resistance of 1817Ω and sensitivity of 9.16 KPa^{-1}. The sensors were reliable with the limit of 400 compression cyclic tests within its working range of 0-60g/cm^2.

Keywords: Water-based carbon ink, coffee ring effect free, textile-based pressure sensor, viscosity, surface tension.

Declaration

I declare that no portion of the work referred to this thesis has been submitted in support of an application for another degree or qualification of this or any other university or other institute of learning.

28 August 2020

Copyright statement

University Library's regulations (see http://www.library.manchester.ac.uk/about/regulations/) and in The University's policy on Presentation of Theses

Acknowledgement

First of all, I would like to give my sincere and deepest gratitude to my supervisor, Dr. Anura Fernando, a respectable, responsible and resourceful person, for spending his valuable time guidance and effort in supporting and helping me with great patience.

I would also like to express my great appreciation to my co-supervisor Dr. Wajira Mirihanage for sharing his knowledge of materials and providing advices for my experiments. I am thankful to Hannah Rampley and David Kenyon for giving me training and advices on use of laboratory equipment, experimental setups. Additionally, I am very grateful to my friends, Sirui Tan, Huixuan Li and Xiulun Ren who were always willing to listen to me when I was upset, they gave me a lot of advices in both experiments and daily life.

Last but not least, l would like to thank my family members for supporting, understanding and encouragements during my MPhil progress. Especially, I am thankful to my parents who gave me endless motivation and support to finish the research work.

Chapter 1 Introduction

1.1 Background

The term “smart-textiles” is derived from “smart materials” which was first defined in in 1989[1]. Smart textile products meet all criteria of high value-added technology which allows the transformation of traditional textile industry to a high-tech, knowledge-based industry[2]. Since textiles can be used as the body’s closest layer, they can act as an actuator and sensor integrating platform to check the physiological signals of the body[3]. These textiles have both good physical properties (such as good flexibility) and the required sensory properties. Because of these advantages, researchers have been working on applying these textiles on garments to monitor physiological signals for healthcare and military since 1998[4]. Smart-textiles are continuing to develop and gradually replacing many of the conventional wearable sensing devices. They have already received tremendous attention due to their potential applications.

Because of the sensing ability of smart textiles, they can be categorised into three groups: passive smart textiles, active smart textiles and very smart textiles [5]. For example, passive smart textiles can be those textiles which can sense the environment [6], whereas active smart textiles can sense the stimuli from the environment and react on it. Very smart textiles can adapt their behaviours to the surrounding circumstances [7]. Because of the ability to sense by intelligent textiles, some physiological data from the body of humans can be measured and recorded[6]. The collected signals are important relating to people’s health, such as heart rate[8], body temperature[9], sweat

content[10] etc. Because of all the advantages and applications mentioned above, many efforts are being put on the development of smart-textiles. Textile pressure sensor is one of the capable applications which can be used to monitor blood pressure as well as heart rate over a long period of time[11][12].

Basic electro-textile sensor structures can be produced using various traditional textile manufacturing methods, for example; weaving, embroidery, knitting, nonwovens and stitching[6]. Usually conductive yarns are available in the form of metal yarn, spun yarn and metal-coated yarn that can be embedded into textile to produce electrical sensor or actuator elements [13][14].

With the development of coating/printing technologies and conductive inks, a range of processes such as dip coating, inkjet printing, screen printing are widely used to deliver additive patterning of ink pigments onto rigid, flexible and comfortable surfaces [15]. The adaptation of functional materials to perform as active pigments within ink formulation has gained an increasing attention over recent years. The property of the conductive inks have huge effects on the accuracy, sensitivity, reliability and durability of the textile sensors[16][17].

1.2 Problem definition

There are various water-based electro-conductive inks available in the market, however, coffee ring effect is commonly found among them. The coffee ring is an unwanted effect for the end use of the inks and is caused by a range of factors, including ink viscosity, wettability of the substrate and solvent vapourisation uniformity [18]. With a low viscosity, it is hard for the ink to maintain stable dispersion and lead to the

undesired coffee ring effect. The most important factor leads to the coffee ring effect is related to the drying process. Coffee ring effect is most possibly caused by the outward flow arising from an unbalanced evaporation from the ink during the drying process [18].Because of the outward flow, the conductive particles are aggregated to the edges of an ink drop during drying [19]. This would lead to un-uniform distribution of the conductive particles on the substrate and further influence the conductivity of the coated fabrics.

Metal inks such as silver and copper inks have low electric resistance, however they tend to be oxidized in the environment easily. It was found from previous research that fine melt-bond nonwoven polyester fabrics dip-coated with silver inks were suitable for the production of textile-based pressure sensors [20], but the oxidization of silver led to short lifetime. Graphene inks have gained much interest but there are still no mature methods to produce graphene inks with small-layered graphene particles and graphene with many layers are not strictly 2D materials and the electric resistance of graphene inks are still high [21]. Activated carbon particles have good electrical conductivity in creating textile-based sensors and would not be oxidized. In this research two solutions were proposed to avoid the coffee ring effect, i.e. increasing the viscosity of the water-based ink and adding co-solvent to create an inward flow during drying process. It was expected to introduce a water-based carbon ink which is free from coffee ring effect for fine nonwoven polyester fabrics by using a formula of different additives such as binders, viscosity modifiers and surfactant in this research.

1.3 Research aim and objectives

1.3.1 Research aim

The aim of this research is to develop a water-based carbon ink, which is free from coffee ring effect based on the Marangoni effect principle for the production of fine nonwoven polyester pressure sensors.

1.3.2 Research objectives

The objectives of this research can be listed as follows:

1) To obtain an optimal viscosity for water-based ink for the prevention of coffee ring effect.
2) To find out a method to create an inward flow (based on the Marangoni effect hypothesis) during drying process to avoid coffee ring effect.
3) To identify optimal particle size, viscosity and surface tension for the impregnation of fine nonwoven polyester fabrics.
4) To figure out the influence of carbon particles distribution on the performance of textile-based pressure sensors.

1.4 Thesis layout

This thesis is composed of six chapters. The first chapter focuses on the introduction of background information of this research. The motivations and aims of this research are discussed. Chapter two regards to the literature reviews related to the conductive ink and wearable textiles. Chapter three describes the principles and details of carbon ink development. This part includes the measurement and adaptation of particle size, viscosity and surface tension of the ink. Chapter four introduces the coating processes of the electro-conductive fabrics including the distribution processes of carbon particles

on the substrate and mechanical behaviors of the substrate before and after coated. Chapter five illustrates the design and manufacture of the wearable pressure sensor. The evaluation of electro-conductivity, sensitivity and reliability of the ink are also introduced. In chapter six, the findings from this research are summarised and recommendations for future investigations are suggested on the results of this research.

Chapter 2 Literature Review

Previous research in the area of electronic-conductive ink formulation, impregnation methods for textile and production of textile-based sensors were reviewed. In this chapter each technology and information and electronic-conductive ink formulation is critically scrutinised based on the aim of the research.

2.1 Electronic-conductive ink formulation

Coffee ring effect is an unwanted effect that should be prevented. In order to make a coffee ring free ink for textile-based sensors, the components must be optimised properly. The following section will focuses on the coffee ring effect and components of electronic-conductive inks, including solvents, conductive particles, binders, viscosity modifier, surfactant and stabilizer. All the research reviewed would be compared with the aim and objectives of this research.

2.1.1 Coffee ring effect

The coffee ring effect is a common and unwanted phenomenon related to inks [22]. The coffee ring effect would lead to conductive materials deposited unevenly on the substrate. There are many factors could cause the coffee ring effect, including ink viscosity, wettability of the substrate and solvent vapourisation uniformity [18]. If the viscosity of the ink is too low, it cannot hold stable dispersion on the substrate and would finally leads to coffee ring effect. However, it is widely accepted that the greatest contributing factor for the coffee ring effect is the solvent vapourisation during the drying process. According to the explanation reported by Deegan [23], when a droplet

is deposited onto a substrate, a contact line would be formed at the droplet-substrate interface. The evaporation rate is typically highest at the edge of the droplet–substrate interface (also known as the contact line) due to the highest surface area to volume ratio. As the evaporation rate at the edge of a droplet is higher than that in the middle, during drying, the contact lines may pin the droplet, so that an outward convection flow would have to be induced from the droplet center to the edges (shown in Figure 1) to replenish the evaporated solvents [24]. This outward convection flow thereby deposits the dispersed material at the droplet edges, leaving little to no material at the droplet center. The nonuniform deposition of functional materials would further influence the final applications, thus there was a need to avoid the coffee ring effect during this research.

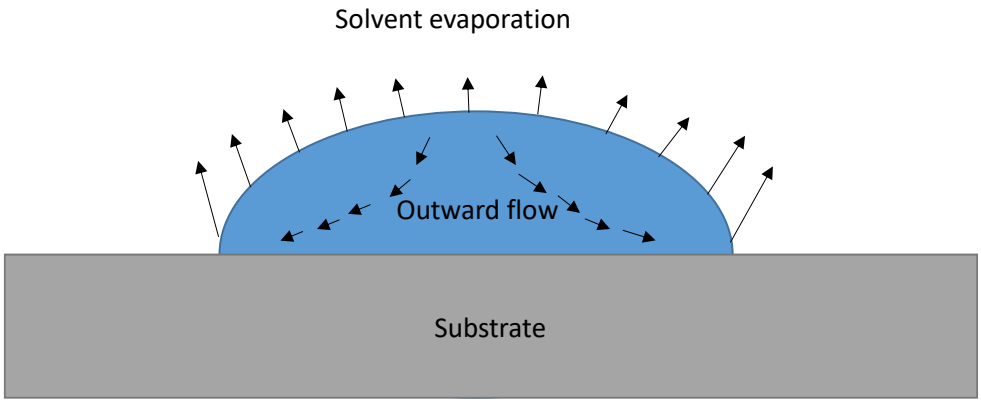

Figure 1. High evaporation at the droplet edges during coffee ring formation [23]

The Marangoni effect is usually caused by the surface tension gradient. As the liquid with high surface tension has more pull on the surrounding liquid than the liquid with low surface tension, the existence of surface tension gradient will naturally lead to the liquid flowing away from the low surface tension area [25]. When there is surface tension gradient shown in a droplet, it will form Marangoni flow under the effect of

surface tension gradient, which makes the liquid flow back to the thin surface along the best route.

In summary, as this research focuses on the development of an ink free from coffee ring effect, the coffee ring effect could be avoid by increasing the viscosity of the ink or creating an inward flow based on the Marangoni effect to balance the outward flow during drying process.

2.1.1 Solvents

Solvents are the diluent to the other ink components like pigments, resins and additives. The primary function of the solvent is to keep the ink in a form a liquid during the coating/printing process before it is finally deposited onto the substrate[26][27]. Solvents can be ranged from variety of organic solvents to water[28].

It has been reported in many researches that N-methyl-2-pyrrolidone (NMP) was widely used as solvent without any further formulations. In Xinxin's research[29] NMP was used as solvent for black phosphorus (BP) ink. In Davide's[26] and Withers's[30] research, NMP was applied for the conductive inks. It has also been reported by Colman that NMP was used as solvent to form conductive ink for thin-film transistors[31]. However, all the researches show that NMP based inks have poor concentration (< 1 g/L) and high boiling point (203℃) which lead to inefficient and time-consuming printing/coating process.

Evolving from the early NMP-based dispersions, printing of solvents with lower boiling point such as alcohols and water emerged[32]. In Juntunen's[33] and Hu's[34] research, Isopropyl alcohol (IPA) was used as solvent to form conductive inks. More evidences

of IPA used as solvent of conductive ink were found from Hasan's[35][36] and Ferrari's[37] work.

There are also some researches about using water as solvent. It was reported by Xu's[38] and Tuantranont's[39] team that water could also be used as solvent for conductive inks. In Torrisi's[40] work, the formulation of conductive ink with water as solvent was further described. It has been proved from all these researches that water is one of the environmental-friendly solvents with low boiling point (100℃). Water has low viscosity (1 mPa.s) and high surface tension (73 mN/m) to be used as solvent for electronic-conductive inks, thus additives are needed.

In summary, water is an environmental friendly solvent, it is safer for the operator during the formulation process. Water is more suitable for substrates with good absorbtion. Compared with NMP, water shows lower boiling point, which means textile substrate impregnated with water-based inks would be easy dried with a low temperature. As the ink developed in this research was aimed to be used on textile substrates, low temperature and less time during drying indicate that there is less possibility that the property of the substrate being influenced during the drying process. Additives would be needed to further optimise the ink.

2.1.2 Conductive particles

Conductive particles play an important role in the conductive inks as they can heavily influence the conductivity of the inks. Generally speaking, the conductive materials used in ink formulation can be divided into three groups: metal[41][42], carbon[43][44] and 2D materials[45][46].

The most widely used conductive materials are metal particles such as Ag, Cu, and Au etc. The preparation methods of metal particles for conductive inks can be divided into two as top-down and bottom-up. Top-down also known as physical methods are usually high-energy methods, in which bulk metal, or microscopic particles are converted to nano-sized particles. Among the top-down methods, the most widely used are physical gas-phase methods based on the rapid condensation of metal vapor usually obtained by thermal heating or plasma excitation of metal plates, powders or wires followed by its transport with a stream of an inert gas (N_2, Ar, He) onto a solid substrate or into a liquid containing a stabilizing agent in order to accumulate, stock, and handle the metal particles[47][48]. This technique was employed for preparation of Ag and Cu nanoparticles (NPs) in the size range from 4 to 80 nm[49]. In bottom-up methods, NPs are built up from metal atoms and nuclei, which are formed either from precursor ions and molecules with the use of a proper reducing agent, or from precursor molecules by their decomposition[50]. There are several evidences of metallic ink used in e-textile. Because of the high cost, gold is not widely used in the manufacture of conductive ink, while silver is the mostly used metal particle. Dearden reported a type of silver ink prepared for e-textile. Preparation of the ink involved the straightforward synthesis of the Ag salt followed by its dissolution in xylene. Ink viscosity for a 16% Ag ink formulation was reported as 4.04 mPa.s with a surface tension of 28 mN/m[51]. There was also a new class of silver complexes obtained by reacting silver oxide, Ag_2O, with ammonium carbamate or carbonate derivatives. In the case of silver 2-ethylhexylammonium 2-ethylhexylcarbamate, its solution in isopropanol was patterned

on a Polyester (PET) film with an inkjet printer[52]. Although silver shows high conductivity, the high cost of it is still a big problem. The main challenge in formulation metallic conductive ink is how to replace Ag by the much cheaper metals, as Cu and Al. There are several researches about the formulation of Cu and Al inks. In early research, Rozenberg adapted Cu (I) chemical vapour dispersion (CVD) precursors as a liquid-phase CVD process[53]. A solution of vinyltrimethylsilane Cu(I) hexafluoroacetylacetonate was inkjet printed directly onto a glass substrate at temperatures below 200 ºC. Copper-rich deposits were formed immediately on impact of the droplet on the heated surface. Porosity of the deposit was evident and caused by the volatile Cu complex as a result of the disproportionation process of the MC precursor. Tetravinylsilane tetrakis Cu (I) 1,1,1,5,5,5-hexafluoroacetylacetonate, (TVST)Cu(hfac), is a solid at room temperature and thus can be stored more easily than liquid copper complex precursors (Figure 2).

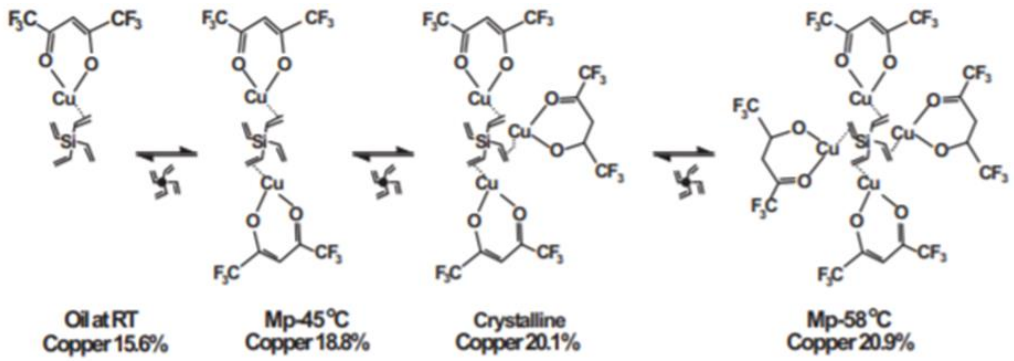

Figure 2. The dynamic equilibrium of (TVST)Cu(hfac) driven by Cu(hfac) to tetravinylsilane stoichiometry[53]

Upon addition of tetravinylsilane, a dynamic equilibrium produces lower unclearity complexes, which are liquids and can be ink-jetted neatly, thereby maximizing the copper content of the ink[54]. Turning to Aluminum ink, Rockenberger's research

refers to a broad range of Al compounds, stabilized with donor ligands and capable of decomposition at temperature around 100 ºC. The process is anticipating the expected use of printing and curing under inert conditions[55]. Al undergoes rapid oxidation in air (~100 picoseconds) with formation of a dense thin amorphous Al_2O_3 layer (2-6 nm)[56][57] that results in loss of electrical conductivity and makes aluminum inapplicable for conductive ink formulations.

The carbon materials are another type of conductive materials and can be used to formulate conductive ink. The two main members of the carbon family are activated carbon and carbon nanotubes. Activated carbon (AC) is a type of specially treated carbon. Organic raw materials (shell, coal, wood, etc.) are heated under the condition of air isolation to reduce the non-carbon components (this process is called carbonization). Then, they react with the gas to make the surface get eroded, resulting in the structure with developed micro-pores (known as activation)[58]. In Mattmann's work[59], carbon particles were used to make conductive ink for yarns. The work was focused on the influences of temperature and humidity on resistance. In Capineri's report[60], it was noted that conductive materials like carbon were attractive and used for sensors. Turning to Guo's report[61], carbon black composite dielectric was used as well to produce conductive ink. Activated carbon is easy-making materials with good conductivity and lower costs.

Carbon nanotubes (CNTs) are one-dimensional quantum materials with special structures (radial size is nanometer, axial size is micron, and both ends of the tubes are basically sealed). They can be divided into two groups: Single-walled Carbon

nanotubes (SWCNTs) and Multi-walled Carbon nanotubes (MWCNT)[62]. There are evidences about carbon nanotubes being used for conductive inks. In Yamada's research[63], conductive ink with CNTS was used to print a thin film. The carbon nanotube thin film presents a large measuring range up to 280%, and it achieves a relatively faster response speed, lower creep and higher durability. It was reported in Han's[64] and Devaux's[65] work that single-walled carbon nanotubes could be used to make inks with high conductivity for yarn coating. Forghoui[66] and his team used CNTS to make conductive ink for yarn coating and used the yarn to make a composite with Spandex to achieve good stretchability and electrically conductivity. It can be found that at the beginning of the formation of the multi walled tube, the trap centre between layers is easy to catch various defects, so the wall of the multi walled tube is usually full of small hole like defects. Compared with multi wall pipe, single wall pipe has smaller diameter distribution range, fewer defects and higher uniformity. However, the manufacture process of producing single-walled carbon nanotubes is still a big challenge. During the production of CNTS, the growth of tube diameter is uneven and the length is not well controlled. Impurities and catalysts are not easy to be removed. It is difficult to control the growth of specific chiral carbon nanotubes. The modification processes are complex, and there are still many defects after modification[67][68].

Among the 2D materials family, graphene based materials have the highest potential to achieve good conductivity for conductive inks[69][70]. Graphene is a type of two-dimensional nano material, which is composed of carbon atoms and SP^2 hybrid orbital and has a hexagonal honeycomb lattice[71][72].It has excellent optical, electrical and

mechanical properties, and has important application prospects in materials, micro/nano processing, energy, biomedicine and drug delivery[73][74]. In Yang's[75] and Wang's[76] work, graphene was used to produce conductive ink for the manufacturing of conductive yarns. The yarns were further used to produce conductive fabrics. The graphene-based yarns showed a linear relationship between strain and resistance. Boland[77] and his team soaked the rubber band in an NMP and graphene mixed ink, after the rubber was treated in toluene for 3.5 h to produce a graphene-rubber composite for body motion detection. There are also many researches based on reduced graphene oxide. Graphene oxide (GO) can be produced by graphite on oxidation; the hydrophilic functional groups can increase the intercalation of water molecules into the graphite; hence the GO sheet can be separated from the graphite. After the GO sheet is produced, the sodium borohydride or hydrazine hydrate can be used to produce reduced graphene oxide (RGO) which is conductive[78]. In Trung's work[75], single reduction graphene oxide was used to produce conductive ink for fibres to manufacture the temperature sensors. Yun's[79] team tried to produce flexible and durable yarns and fabrics wrapped with RGO. BSA proteins were used as the adhesives for increasing the absorption of GO onto yarns and fabrics. By using this method, they manufactured RGO materials based on nylon, cotton, nonwoven and polyester. Other 2D materials have their own advantages, but they are not suitable to be the conductive materials in inks. Hexagonal boron nitride (h-BN) is mostly used as lubricant[80][81] or dielectric and thermally conductive filler[82][83], the use of MOS_2 is mainly based on its low coefficient of friction[84]. The potential applications of black

phosphorus(BP) is in optoelectronics and photonics[85][34].

In summary, metallic materials have the highest electro-conductivity, however, the oxidization of them is a big problem. Although the oxidation of Cu NPs is less rapid compared to Al NPs, it still leads to a bad influence in its conductivity. Metals can avoid oxidization such as gold and platinum are too expensive. As this research aimed to develop an ink for wearable textile-based sensor, the lifetime should be put into consideration. As textile-based sensor would be exposed in the open environment, because of the oxidization and short lifetime of metal particles, they were not suitable choices for this research. Activated carbon is a material with good electro-conductivity and can be produced easily. CNTS have better electro-conductivity than activated carbons, but the modification processes are complex and are of high cost. Graphene is the material with the best electro-conductivity within the 2D materials family. The electro-conductivity of graphene is based on the number of its layers, the less the layers the better the electro-conductivity. However, due to the strong cohesive force between the graphene sheets in the graphite, there are still no stable methods to produce single-layered or few-layered graphene inks. Graphene with many layers have much less conductivity than other electro-conductivity materials mention in this part. As the ink was aimed to be used to produce textile-based sensors, the electro-conductivity should be good, graphene was not chosen because graphene with many layers showed bad electro-conductivity. Activated carbon was suitable for this research because it met the aim of producing ink for textile-based wearable sensors. Activated carbon particles showed good electro-conductivity, thus they can be used to create sensors. They will

not be oxidized, thus they are suitable to be used on textiles-based sensors which would exposed to the environment in this research.

2.1.3 Binders

Binders (also known as binder portion) are added to the ink to “bind” the pigments together and provide adhesion of the pigments to the substrate. Acrylics, alkyds, cellulose and its derivative, and rubber resins are commonly used as binders[26]. Some types of binders can also contribute to the properties of the final products. The influences include: affecting gloss, resistance to weathering, and chemical attack or abrasion. Xanthen gum is a type of binder which was widely used in food and medical industry. It has unique rheology, good water solubility, stability to heat and acid and alkali, and good compatibility with a variety of salts. It has been reported that high glass transition temperature polymers such as polyimides allow resistance to high temperature[27]. Water insoluble polymers such as cellulose can provide resistance to moisture. It has also been further reported that cellulose can lead to a huge increase in the viscosity of the ink. However, cellulose-based binders required high temperature (300℃) drying, which would influence the property of textile-based substrates, thus it is not suitable for the aim of producing ink for textile-based sensors.

In summary, Xanthan gum was a good choice to be the binder in this research. This research aimed to produce water-based ink, Xanthan gum shows good water conductivity and biocompatibility. It can also be easy dried after the impregnation process, which also meets the aim of producing an ink for textile-based sensors.

2.1.4 Viscosity modifiers

Viscosity modifier is one of the additives that can be used to adapt the viscosity of inks. Ink viscosity is a key consideration in suiting the final coating/printing process[87]. Some processes like screen printing require viscous ink while some others like screen printing need high fluent, low viscosity ink. Rheology is used to describe the property of a fluid over time and shear stress and shear strain, viscosity refers to the interaction of shear, shear stress and shear strain of a fluid at a certain point of time[88][89]. An applied shear stress can cause influence to the rate of flow which determines the viscosity[90][91]. As shown in Figure 3 below, the liquid can be regarded as a cube of fluid. A flowing liquid will show a velocity gradient perpendicular to its rate of flow. The unit of the gradient in flow velocity is $\frac{m/s}{m} = s^{-1}$ and is named as shear strain or shear rate[92].

(A) (B)

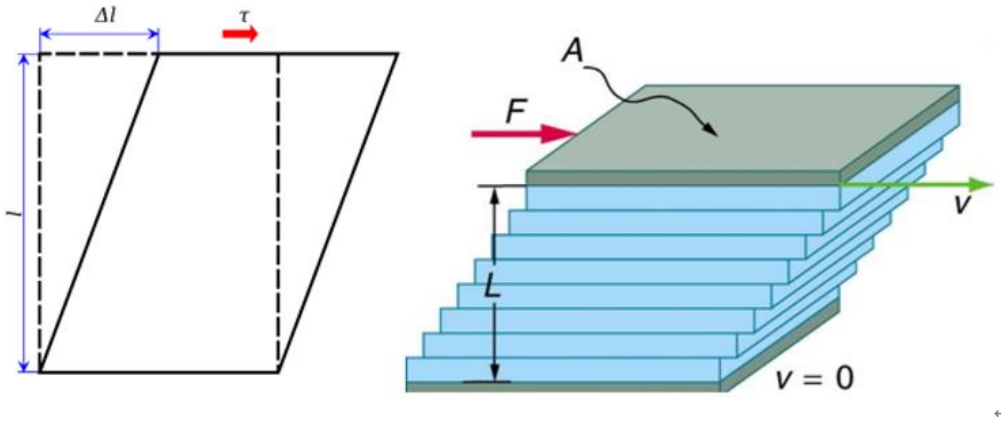

Figure 3. Laminar flow of liquid under shear (A) Shear stress and shear strain (B) Multi-layered liquid flow under constant shear[92]

Shear stress is defined as the force per unit area of liquid, unit used for it is N/m^2 (=Pa). Formally, viscosity (represented by the symbol η "eta") is the ratio of the shearing stress (F/A) to the velocity gradient ($\Delta v_x/\Delta z$ or dv_x/dz) in a fluid. It is represented

as $\eta = \frac{F/A}{\Delta vx/\Delta z}$ or $= \frac{F/A}{dvx/dz}$. The SI unit for viscosity is pascal second [Pa s], which has no special name[93][94]. What should be mentioned is that there are many unit systems used for viscosity. One of the units that are most commonly used nowadays is the dyne second per square centimeter (dyne s/cm^2), which is given the name poise (P) after the French physiologist Jean Poiseuille (1799–1869). Other units used are 'milli Pascal seconds' (mPa.s), centipoise (cP), and Stokes (S) as well as centiStokes (cS).

Based on the rheology of an ink fluid, the flows can be generally divided into two groups: Newtonian fluid[95] and Non-Newtonian fluid[96].

Newtonian fluid also known as ideal fluid is a fluid where the viscous stress arises with a linear proportional to its strain rate. Because of this the viscosity of a Newtonian fluid will not change with its shear rates[97][98]. Newtonian fluid is the simplest mathematical models of fluids used for viscosity. However, in the real world there are no fluids fit this model perfectly, the closest ones are water and solvent or mineral oils, they can be considered as Newtonian fluids[99]. Figure 4 below shows the relationship between shear stress and viscosity and shear rate for different fluids.

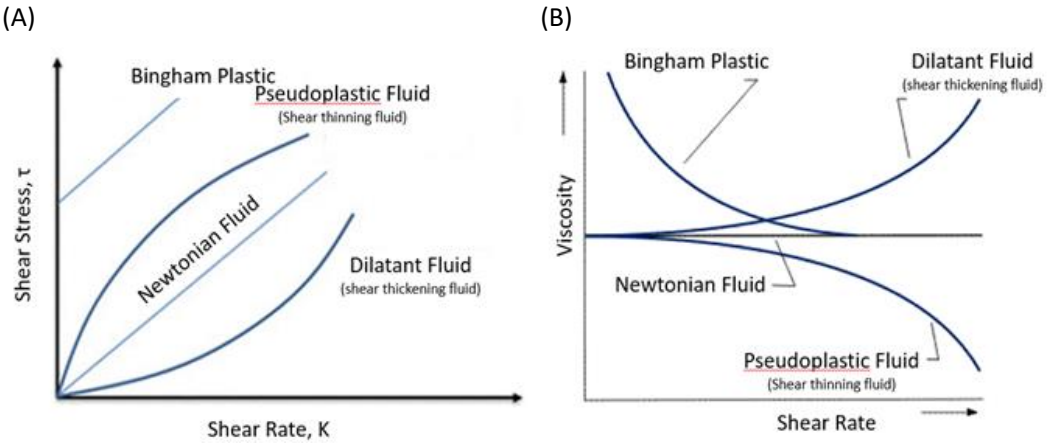

Figure 4. Property of different fluids(A) Relationship between shear stress and shear rate for different fluid systems (B)Viscosity and shear rate for different fluid systems[103]

Most of the fluids (especially inks used for coating/printing) are Non-Newtonian fluids. Unlike Newtonian fluids, their viscosity can change when under force to either more liquid or more solid[100]. Based on how the viscosity changes under different shear rates, Non-Newtonian fluids can be divided into several groups which are: pseudoplastic (shear thinning)[101], dilatant (shear thickening)[102], viscoplastic (Bingham fluids)[102], thixotropic and rheopectic[103] (shown in Figure 4). The interactions between the components of a fluid system and the mechanical phenomena determine how the fluid behaves. The behavior of different fluids under different shear rates will be mentioned below:

Pseudo plastic fluid is also known as the shear thinning fluid. The shear stress of the fluid decreases as the shear rate increasing, which represents as a drop in viscosity. Because of entanglement of powders and small particles in the system, shear-thinning liquids have a viscous and pasty structure. While shear is applied to the liquid, the components in the fluid can stretch and disentangle which allows them to slip past another. For some circumstance, shear thinning is required as it not just allows the flow

go through some high shear elements but also prevents the ink from moving or smudging once it is deposited in a substrate.

The viscosity of shear-thickening fluid increases with the increasing of shear rate. Generally, shear-thickening fluids are highly concentrated suspensions in colloidal form. The reason for shear-thickening is that the liquid components entirely wets the solid components in the fluid which causes a low viscosity, while the shear rate increases, the particles can interact readily to form a solid structure inside the fluid to increase the viscosity[27].

Viscoplastic fluid does not flow as a certain threshold is reached. Some fluids with this property are toothpaste in a tube and tomato ketchup[104]. The reason for this is that in the viscoplastic fluid a certain amount of shear stress is required to overcome the inter-particle/inter-molecular binding force to let the liquid flow.

Bingham plastic is a certain type of viscoplastic fluid, it behaves as a rigid body at low stresses but flows as a viscous fluid under high stress. It is named after Eugene C. Bingham who proposed its mathematical form[105]. The model of Bingham plastic is commonly used in drilling engineering for mud flow or in the in the handling of slurries. One typical example of Bingham plastic is the toothpaste.

There are several methods (like using mixers or blenders) widely used all over the world to measure the viscosity of inks. For shearing rheometers there are four basic shearing planes can be defined according to their geometry:

- Couette drag plate flow
- Cylindrical flow

- Poiseuille flow in a tube and
- Plate-plate flow (cone-to-plate methods)

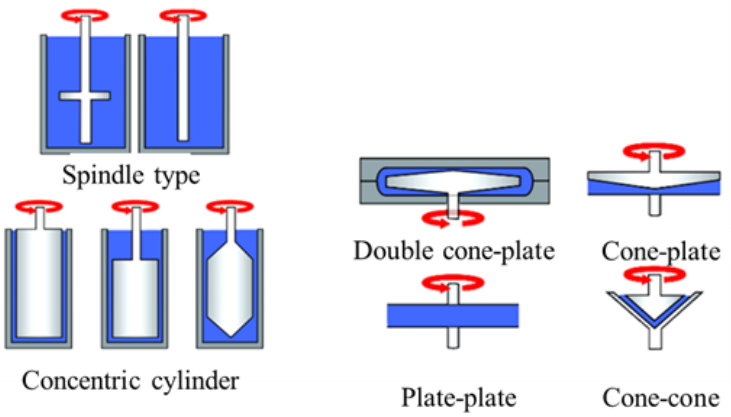

Figure 5. Rotation geometries of different types of shear rheometers[103]

Among them the most expensive ones are plate-to-plate and cone-to-plate methods. Although the two methods are expensive, they are the most accurate ones and can offer information about the rheological performance of non-Newtonian fluids with high quality. The plate-to-plate method is one of rotation-based rheology measurement methods. In this method, a controlled shear rate or shear stress is measured and delivered to the fluid to examine the fluid's viscosity over a period of time.

Cone-to-plate (CTP) and plate-to-plate (PTP) rheometers are the most complicated methods available to measure the viscosity of inks. The principles used for CTP and PTP are shown in Figure 5. In CTP, a conical top plate is used to make sure that the shear rate is constant across the whole plate. In PTP, a flat top plate is used. During the measuring process, sample fluid is added into the gap between the two plates and certain shear rate is added to measure the viscosity. PTP rheometer is more suitable for inks with large particle size. It is easy to manufacture and can operate with bigger plate gaps.

However, it may suffer from the inaccuracy caused by the different shear rates across the plate face. Turning to CTP, it requires more accurate machining of the cone. Because of the small gap in the center it is more suitable for inks with small particles. Both equipments are highly useful for the measurement and understanding of the rheological behavior of fluids and help a lot during the ink formulation process[106][107]. They can be used to analyze fluid behaviours such as shear-thinning and shear-thickening.

In summary, as this research aimed to produce a water-based carbon ink which was free from coffee ring effect, viscosity modifiers were needed to adapt the viscosity of the ink. Guar gum could be a suitable choice for its good water solubility, it is also harmless to human body during the formulation of the ink or after being applied to textile substrates.

2.1.5 Surfactants

Surfactant has two main functions: control the surface tension of the ink and stabilize the functional particles within the conductive inks. Surfactants can adsorb onto the surface of conductive materials, promoting their stabilization in the solvents[108]. This strategy can support higher concentration of stabilized conductive particles in the liquid environment. There are two types of surfactant widely used nowadays, ionic surfactants and non-ionic surfactants.

Among the ionic surfactants, it has been found that some of the effective surfactants are facial amphiphiles[109] (i.e. molecules with a quasi-flat molecular structure with hydrophobic and hydrophilic faces), for instance bile salts such as sodium cholate (SC) [110]and sodium deoxycholate[40]. When such ionic surfactants and conductive

particles interact in water, the surfactant molecules are adsorbed onto the surface of the particles, generating temporary effective charge[37]. The induced charge around can generate a Coulomb repulsion which further prevents re-aggregation[29]. The required concentration of an ionic surfactant for stabilization can be estimated by surfactant critical micelle concentration (CMC), which is typically determined by the critical surface tension of its solution against concentration. Below CMC, further addition of the surfactant causes a great change in the surface tension as the surfactant molecules assemble at the solution–air interface. Above CMC, the interface is saturated where the surfactant molecules spontaneously arrange into micelles, so that further addition of surfactant causes minimal changes. Another parameter should be mentioned is the Hydrophile-Lipophile Balance Number (HLB)[111]. HLB was first determined by W.C. Griffin in 1949. The HLB value is used to explain the equilibrium relationship between hydrophilic groups and lipophilic groups in surfactant molecules. The lipophilic or hydrophilic degree of surfactants can be determined by the size of HLB value. The larger the HLB value is, the stronger the hydrophilicity is. The smaller the HLB value is, the stronger the lipophilicity is[112]. In Griffin's report the HLB for surfactant was set between 0 and 20, the HLB value of paraffin wax which is composed of saturated alkanes with the largest hydrophobicity was set as 0, and the HLB value of polyoxyethylene which is composed of hydrophilic oxyvinyl group was set as 20 [111]. In recent years, with the continuous emergence of new surfactants, more hydrophilic varieties have been used in practice, such as sodium lauryl sulfate HLB value of 40 [112].

Turing to the non-ionic surfactants, typical non-ionic surfactants include Triton-X, Tween and Brij series, and polymers such as sodium carboxymethylcellulose (Na-CMC), polyvinylpyrrolidone (PVP) and ethyl cellulose. The polymers can attach onto or encapsulate the conductive particles and provide a physical separation between them. Liang et al. demonstrated the addition of ethyl cellulose in ethanol for exfoliation and stabilization of graphene flakes using this strategy[113]. The authors suggested that the cellulose created a colloidal dispersion and prevented the graphene flakes from aggregation. Polymers are of particular interest for subsequent ink formulation as they can function not only as binders but also can be used to tune the physical properties of the inks for relevant printing technologies[114]. In another research, 1-pyrenesulfonic acid sodium salt (PS1) was used as surfactant[115]. However, it has been reported in the same research that PS1 did not behave as a traditional surfactant as it did not accumulate to the surface, only very high concentrations (much more than 0.5 mg/ml) could cause changes in surface tension. Comparing all the surfactants reviewed, it can be concluded that non-ionic surfactants have high stability and are not easy to be affected by the presence of strong electrolytes or by the influence of acids and bases. As this research aimed to produce a water-based coffee ring effect free ink, many additives would be needed, the stability of non-ionic surfactants made them suitable for this research. Among the surfactants reviewed, Triton X-100 shows good solubility in water and ethylene glycol which made it a good choice under the aim of producing water-based ink.

2.2 Substrates

The substrate materials used for electro-textiles are still based on traditional textile materials such as cotton, wool, Nylon and polyester. Textile structures include knitting, weaving and nonwoven are used to form the substrate. The selection of substrate materials and structures is based on the final applications.

2.2.1 Substrate materials

Materials used to produce substrate yarns/fabrics are still traditional textile materials. Cotton, wool, polyester and nylon are four of the mainly used textile materials.

Unlike normal bast fibre, cotton fibre is the seed fibre formed by the elongation and thickening of the epidermis cells of the fertilized ovule. The main component of cotton fibre is cellulose which is a type of natural polymer compound. The cellulose content of normal mature cotton is about 94%. Because of the high content of cellulose, cotton shows high hygroscopicity. Under normal conditions, the cotton fibre can absorb water from the surrounding atmosphere with a moisture content of 8-10%[116]. Because cotton fibre is a bad conductor of heat and electricity, its thermal conductivity is very low, and because cotton fibre has the advantages of porosity, a large amount of air can be accumulated between fibres, air is a bad conductor of heat and electricity. Therefore, pure cotton fabric has good warmth preservation[117]. Because of the good hygroscopicity, cotton is commonly used in coating/printing. In Alex's[118] and Jun's[119] researches, cotton was coated and made into sensors. The "Moisttech Corp"[120] also developed a cotton-based moisture sensor. However, although cotton fibre can achieve a high take up rate, the wrinkle resistance and tensile property of

cotton are very poor, which makes cotton not suitable for mechanical force sensor. As this research aimed to produce pressure sensors, cotton may not be a good choice.

Wool is mainly composed of protein. It has the advantages of good elasticity, hygroscopicity and warmth retention. Wool is a long and thin solid cylinder, which is curly. There are three layers in wool fibres, named scale layer, cortex layer and medulla layer. However, the scale layer makes it to get wool coated/printed. Wool is not commonly used to produce coated/printed conductive yarn/fabric.

Polyamide, known as nylon in textile, is a general term for polymers containing amide groups in the main chain repeating unit of macromolecules. The most outstanding advantage of polyamide fibre is that its wear resistance is superior to other fibres, followed by its good elasticity. Its elastic recovery rate is comparable to that of wool, and its weight is light, with a specific gravity of 1.14[121]. Nylon was used in many textile sensors. Lee [122] and his team used nylon for a textile strain sensor. Other researches like Colye [4] and Tushar [123] also used nylon for strain sensors. It can be concluded that nylon is mainly for the production of strain sensors due to its high stretchability. The disadvantage of polyamide fibre is that its optical rotation resistance is slightly poor. If it is exposed to sunlight for a long time outdoors, it is easy to turn yellow and its strength is reduced. Compared with polyester fibre, its shape retention is poor and the fabric is easily wrinkled, as the fiber used in this research was aimed to be used to produce sensor the disadvantages make nylon mot a good choice for this research.

Polyester (PET) fibres, is a type of synthetic fibre made of polyester by

polycondensation of organic binary acid and binary alcohol. Polyester fibre has a series of excellent properties, such as high breaking strength and elastic modulus, moderate resilience, excellent heat setting effect, good heat and light resistance. In Zhang's[124] work, polyester was used to produce pressure sensor. It can also been found in Lafleur[125], Kim[126], Pan[127] and other researchers' work that polyester was used for textile sensors. In Yuhua's work, a textile-based pressure sensor was produced using fine polyester fabrics as substrates. Polyester fibres showed good mechanical property for pressure sensor and good conductive ink absorbtion which meet the goal of producing textile-based pressure sensor.

2.2.2 Substrate structures

The production of substrates for electronic textiles is still based on the commonly used textile structures include: knitted structure, woven structure as well as nonwoven structure.

In woven fabrics, two sets of yarns (weft and warp yarns) are interlaced at right angles. Woven fabrics for sensors are generally produced by inserting the electronic conductive yarns[128]. Plain weaves, atlas weaves and twill weaves are the most common and simple woven patterns to manufacture sensing fabrics. Different woven structures have influence on the final performance of the sensing fabric, especially its mechanical properties. Plain [129] is the simplest and tightest weave pattern among all of the structures of woven fabric; the weft yarn passes through the warp yarn alternatively in this structure. The plain weave has the maximum number of binding points which can strengthen the structure and make the fabric robust and tight[130]. It also has more snag

resistance; however, plain-woven structures generally wrinkle more and have lower tear strength.

Atlas weaving (also known as satin weaving)[131] is produced by four or more weft yarns floating over a warp yarn and four warp yarns floating over a weft yarn. Because of the floating yarns within the structure, atlas weaving is looser than the plain weaving structure. This structure is suitable for inserting the conductive yarns into the structure to produce sensing fabric. However, the floats snag easily which leads to a lower durability.

The twill structure[132] is repeated in that the weft yarn passes through one or more warp yarns, and then under two or more warp yarns. Twill woven fabric is strong and durable; it has more wrinkle resistance and is more resistant to soiling, but the cost of the fabrics is relatively higher when compared to that of the other two woven structures[133]. Stoppa's research[134] pointed that the complex network present in woven fabric structures can be used as elaborated electrical circuits integrated with significant electronic components and conductive yarns. In Rothmaier's report[135], a pressure sensitive textile sensor was developed by integrating thermoplastic silicone fibres into atlas and plain-woven fabric. However, only a few yarns are rised from the bottom to the top; hence, there were few resistance changes caused by micro bends when the yarn moves from the bottom to the top. It can be concluded that woven fabrics have high elastic recovery, but the low flexibility and lower tear strength are issues that need to be addressed.

Knitting technology is the fabrication process of combining the loops of yarns to create

the fabric[136][137]. Yarns are delivered to the needle bed and interlaced with each other in the knitting machine. In Li's research[138], a knitted pressure sensor was produced. The electrical resistance of manufactured sensors changes when the pressure decreases due to the twisting of fibres in the space layer and to more conductive connections. In Pavelli's work[139], another knitted sensor was manufactured to monitor physiological and biochemical variables. It can be found that knitted fabrics have high tear strength, permeability and elasticity. Meanwhile, the thickness and bending modulus of the knitted fabric are relatively higher and the dimensional stability lower than the woven fabric[140]. In summary, knitted structure is a suitable fabrication method to create a wearable sensor that tightly fits the body, and it can also provide a comfortable and elastic property for wearers, thus the knitted structure was more suitable for the production of strain sensor.

Nonwoven fabric is a type of fabric which does not need spinning and weaving. It is made of short textile fibres or filaments arranged randomly or directionally to form a fibre-based net structure, and then reinforced by mechanical, thermal adhesive or chemical methods[141]. Nonwovens break through the traditional textile principle, and have the characteristics of short technological process, fast production speed, high output and low cost. There are four main nonwoven technologies used nowadays: spun-bond, melt blown, wet and spun-bonded melt blown spun-bonded (SMS).

Spun-bond nonwovens[142] are made by extruding and stretching the polymer to form continuous filament and then laying it into a web. The web is then made into nonwovens by self-bonding, thermal bonding, chemical bonding or mechanical reinforcement. In

spun-bond nonwovens, polypropylene (PP) spun-bond accounts for about 70% of the total, followed by polyester spun-bond accounts for about 18%, nylon spun-bond and a small number of functional spun-bond. Spun-bond nonwovens are widely used in household products, packaging products, decoration industry, agricultural cloth, waterproof materials, high-grade breathable (wet) waterproof material base cloth, filter materials, insulation materials, electrical appliances, reinforcement materials and other fields.

Melt blown nonwoven is a type of micro-fibre nonwovens, which is made of strong hot air. Its diameter is about 2 microns, and it is the thinnest of all fibres. Because of its special structure and raw material polypropylene, melt blown nonwovens have good water-proof and air permeability, high filtration efficiency, bacteria collection and isolation, poison filtration, heat insulation, heat preservation, insulation, non-toxic, non-stimulation and other functions. Melt blown nonwovens can be used in air filter materials, blood filter materials, battery separator and filter materials, oil absorption materials, thermal insulation materials, other health material markets such as dishcloth and so on[143]. In Yuhua's research, fine nonwoven polyester fabrics was used to produce textile-based pressure sensors [21].

SMS composite nonwovens are the earliest and most active products in nonwovens composite products. The highlighted characteristics of these products include non-toxic, tasteless and highly effective bacteria isolation. Through special treatment, anti-static, anti-alcohol, anti-plasma, water repellent and other properties can also be provided. SMS composite nonwovens are mainly used for high-efficiency filtration materials,

high-efficiency oil absorption materials, medical and health labor protection products such as surgical clothing, surgical caps, surgical protective clothing, hand washing clothes, handbags, surgical instrument sets, as well as thermal insulation materials and clothing accessories[144].

Wet process Nonwovens Technology is to loosen the fibre materials placed in the water, at the same time, make different fibre materials mixed into fibre suspension slurry, the suspension slurry is transported to the mesh forming mechanism, and then the fibres in the wet state form the mesh and then reinforce into cloth. This technology is a new technology to produce wet nonwovens or paper cloth composites by using papermaking equipment and technology[145].

In summary, one of the goals of this research is to produce textile-based pressure sensor. Fine nonwoven materials could thoroughly absorb electro-conductive materials and induce resistive signal actively to pressure changing (even the very small cardiorespiratory signals) which meets the aim of producing pressure sensors being used on human body. Furthermore, nonwoven fabric shows isotropous mechanical properties which is beneficial for the end use of textile sensors after ink are coated on it.

2.3 Impregnation methods

Impregnation of the substrate materials is the essential process in the ink based micro-electronic technology and have been widely investigated and well developed over decades. Five methods are mainly used nowadays to print/coat the ink on substrates.

2.3.1 Dip coating

Dip coating is a type of self-metered method[146] and is commonly used for coating continuous objectives that are not flat, such as fibres and other irregularly shaped discrete objectives[147]. The substrate is usually dipped into the coating solution. In dip coating, the substrate passes under an applicator roll and then submerged in a tank full of coating fluid[148]. During the dip coating process, the prepared substrate needs to be immersed into the solvent/colloid bath thoroughly and withdrawn from it at a specific speed in order to achieve required coating concentration and thickness. Depending on the type of solvent and substrate, the curing process is necessary[149][150]. By using the method of applying electrostatic forces, drops of the coating at the bottom of the dip coated substrate can be removed. There are several researches about using dip coating to produce electro-textile materials. In three-dimensional silver nanowire sponge structure was created using dip-coating technology, which combined the high electrical conductivity with the sustainable mechanical properties of cotton[151]; other cotton based electro-conductive fabrics were also developed using dip-coating technology[152][153]; wool fabrics were treated with electro-conductive solvent as well in order to obtain electro-conductivity[154]. Electro-textile based interconnectors can also be produced by dip-coating[155]. The wet thickness is usually determined by the fluid properties as well as the coating speed[156]. If one tries to coat too fast, air gets entrained under the coating and the coating quality suffers greatly[157]. The suitable viscosity for dip coating is from 50 to 1000 mPa.s [24].

2.3.2 Ink-jet printing

Inkjet printing is a digital, non-contact printing technique where the ink droplets are jetted and deposited in a rapid succession onto the substrate to generate an image[158] [159]. Generally speaking, there are two prevalent droplet jetting mechanisms for inkjet: continuous inkjet (CIJ) and drop-on-demand inkjet (DOD)[160]. CIJ is a process where a stream of ink droplets is continuously generated and jetted. The droplets charged by the electrode are subjected to an electrostatic field and selectively deflected to deposit onto the substrate[161]. On the other hand, DOD is a process where the ink droplets are only generated when demanded through a piezoelectric or a thermal inkjet process[162]. Among the two methods mentioned above, the complexities in controlling of the jetting, deflecting and recycling of the inks have limited the widespread application of CIJ. Due to its simpler operation, DOD has therefore emerged as the main inkjet printing technology. In the DOD process, a key requirement is a stable jetting of single droplets under each electrical impulse without the formation of satellite droplets. The satellite droplets can lead to ink deposition on untargeted areas and even deviation from the droplet jetting trajectory[22][163].

Many researches of using conductive inks for inkjet printing have been carried out. O¨hlund[164] indicated in the thesis that the roughness of the substrate surface was the most important feature in terms of inkjet printed conductive materials. It has been reported that NMP based dispersions of graphene [78] and h-BN were already used for inkjet printing on paper[165]. Torrisi's[166] work showed that self-assembling of bis(trimethylsilyl)amine could lead to a more uniform distribution of graphene flakes.

Hu demonstrated a binder-free, stable BP ink formulation using a mixture of IPA/2-butanol solvents for inkjet printing. Hexamethyldisilazane treatment[167][168]was used to reduce the surface energy of the substrate, thereby reducing the roughness of the printed film. In this way, silver nanoparticles were deposited onto the cellulose film substrate in order to create an organic transistor[169]. Li introduced a flexible capacitor on a polyester substrate fabricated by inkjet printing technology[170]. It had been concluded that the particle sizes plays an important role in inkjet printing[171]. If the particle size is too big, nozzle of the printers could be clogged. The inks for inkjet printing are usually of low viscosity, the drying of low viscosity inkjet inks may lead to coffee ring formation if they are not optimised. How to avoid satellite droplets is another big challenge. As inkjet printing has many disadvantages and challenges to overcome, it was not the best impregnation method suitable for this research.

2.3.3 Screen printing

Screen printing is a stencil process whereby ink is transferred on to the substrate through a stencil screen made of a fine, porous mesh of fabric, silk, synthetic fibres or metal threads[22][172]. The pores of the mesh are closed in the non-printing areas by a photo-polymerised resin, while the remaining pores in the printing areas are left open to allow ink to flow through. Flat-bed screen printing is the most widely used screen printing methods. During printing, the ink is first spread over the screen mesh. A squeegee is then drawn across it, forcing the ink through the open pores. At the same time, the substrate is held in contact with the screen to receive the ink. Many flat-bed screen printing systems still consist of a simple hand-operated unit, which can be useful

for very thick or thin substrate[24][173][174]. Thread count of the screen, the thread diameter, the pressure, the angle that in turn defines the area of the squeegee in contact with the screen, and the speed of the blade in respect to the screen during ink deposition are the factors which influence the amount of ink used during screen printing[175][176][177].

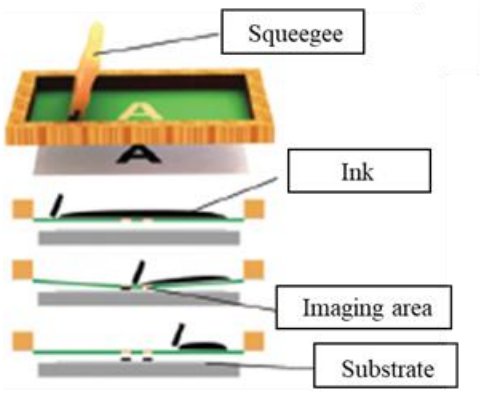

Figure 6. Principle of screen printing[225]

There are several researches about using screen printing for smart applications. In Zhang's work[41], RGO terpineol/ethyl cellulose based ink was used. The authors used this ink to develop counter electrodes for dye-sensitised solar cells (DSSCs). However, this RGO screen ink required a 400℃ treatment to effectively burn off the binder, adversely affecting the adhesion of RGO to the substrate. Other researches Polyvinylpyrrolidone (PVP)/polyvinyl acetate (PVAc)[178][179], Polyaniline (PANI)[180][181] based conductive inks for screen printing. Inherent issues with alternative polymerssuch as the graphene/PVP/ polyvinyl alcohol (PVA) ink[182], which required highly controlled heating processes to achieve pseudoplasticity. It had been proved that the demonstrated pseudoplasticity, although eventually shear thinning, was not ideal for screen printing due to the lack of flow (i.e. too high viscosity). It was

prone to damaging the screens when not under shear [183]. It was found that screen printing needs inks with very high viscosity (more than 1000 mPa.s under shear rate from 1/s to 1000/s)[184][24].

2.3.4 Gravure and Flexographic printing

Gravure printing is a form of “direct” printing upon which ink is carried directly from the ink trough to the substrate via the gravure roller which not only meters the wet ink application weight but also acts as the print image carrier[185]. The printing unit of a gravure press consists of an ink trough in and a metal doctor. The desired pattern is directly engraved into the metal gravure roller in the form of cells which are designed to get filled with ink as the roller rotates in the ink. Ink transfer is achieved by passing the substrate between the gravure roller and an impression roller[186]. Gravure printing process can be divided into four phases: (1) the inking phase at the ink trough; (2) the doctoring phase where the ink is metered by the doctor blade; (3) the printing phase where the substrate meets the gravure roller; and (4) the setting phase when ink is successfully released from the cylinder cell to complete the print[187][188]. The principle of Flexographic is similar to that of gravure printing[189]. Flexographic printing uses a slightly more convoluted ink transfer process. To form an image, soft and flexible relief printing plates are mounted and registered on a plate cylinder. Ink is first applied to the surface of a screened anilox roller[190], which is rolled through an ink trough to fill the cells with ink. The anilox roller is a hard cylinder with engraved cells. Any excess ink is then screened off via a doctor blade. The ink is then transferred to the relief printing plate mounted on a second cylinder before the ink is deposited onto

the final substrate[191][192].

The researches about using conductive ink for gravure printing was firstly carried out by Secor's team in 2014[193]. The researches exchanged graphene from ethyl cellulose/ethanol into ethyl cellulose/terpineol/ethanol for ink formulation, where the loading of graphene and ethyl cellulose was controlled to suit gravure printing. In Baker's report[194], a graphene/sodium carboxymethyl cellulose (Na-CMC) ink in IPA solution was developed and used for flexographic printing. In a most recent research reported by University of Cambridge, a type of conductive carbon-graphene ink was produced for flexographic printing. The ink was then printed on paper and PET. The measured electro-resistance was 16.5 kΩ/sq and 11.5kΩ/sq for paper and PET[195]. It can be concluded that both methods require the conductive ink to be with medium viscosity (100-1000 mPa.s for gravure printing and 1000-2000 mPa.s for flexographic printing) and low boiling point to allow rapid ink drying[196][197].

Comparing with all the different impregnation methods, it can be found that screen printing, gravure and flexographic printing are more suitable for the applications of textile-based capacitors or strain sensors based on the piezo-resistive effect which could not meet the aim of producing pressure sensors in this research. Inkjet printing still has many disadvantages and challenges to overcome, which makes it not the best impregnation method in this research. While dip coating is a simple and efficient technology which has been proved to be suitable to produce fine nonwoven polyester textile-based pressure sensors, thus dip coating was chosen to be the impregnation method in this research.

2.4 Wearable sensors

Wearable sensors can change their electrical properties according to the environmental impact. Three different types of wearable sensors are mainly used nowadays.

2.4.1 Piezoelectric sensors

Piezoelectric effect (Figure 7) is the principle behind this type of sensor. Piezoelectric effect represents the ability of certain materials which can generate an electric charge in response to applied mechanical stress[198]. The piezoelectric effect is unique and reversible, which means the materials can exhibit both direct piezoelectric effect and converse piezoelectric effect. The piezoelectric effect is very useful within many applications that involve the production and detection of sound, generation of high voltages, electronic frequency generation and microbalances[199].

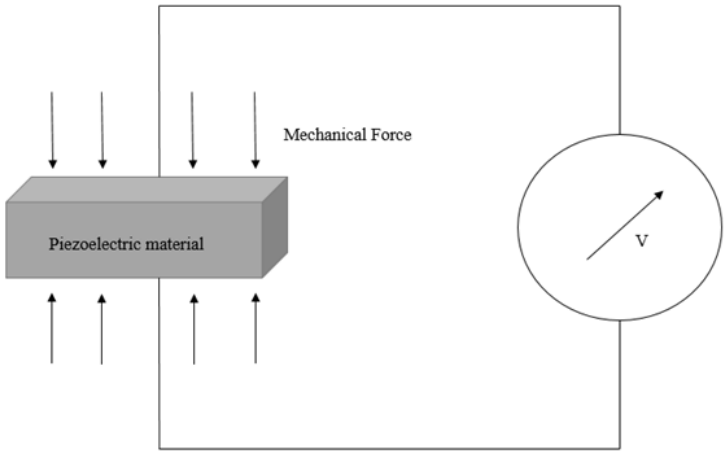

Figure 7. Principle of piezoelectric effect[226]

There are many materials, both natural and man-made, exhibiting a range of piezoelectric effects. Some naturally piezoelectric occurring materials include Berlinite (structurally identical to quartz), cane sugar, quartz, Rochelle salt, topaz, tourmaline, and bone (dry bone exhibits some piezoelectric properties due to the apatite crystals,

and the piezoelectric effect is generally used to act as a biological force sensor). Example of man-made piezoelectric materials include barium titanate and lead zirconate titanate[200]. However, when it comes to flexibly sensors which should be portable and wearable, the focus is put on polyvinylidenefluoride (PVDF). There are some evidence found about PVDF used in sensing application: in Jiang's work a PVDF based flexible sensor was created for cardiorespiratory sensing. It was found that extra encapsulation was needed to eliminate the bending artefacts[201]. Kevin Magniez and co-workers from Deakin University and CSIRO in Australia, and RWTH Aachen University in Germany[202] found that thin piezoelectric polyvinylidene fluoride fibres containing a high piezoelectric β-phase content of up to 80% can be used for melt spinning. It was reported that after crystallization from the melt, the fibres were subsequently stretched uni-directionally at 120°C between 25 and 75% of their original length, and can be made into a stretch sensor using weaving technology [203]. However, one of the disadvantages of piezoelectric sensor is that it is vulnerable to noise and motion artifacts. There is an essentially requirement of extra shielding processing or data filtering algorithm for such sensors. Because this research aimed to produce ink for textile-based wearable sensors, there could be many noises or motion artifacts during real applications, as piezoelectric effect is sensitive to them, it could lead to inaccurate results during the research.

2.4.2 Capacitive sensors

Another principle used for e-textile is the capacitive sensing. Generally speaking, capacitive sensor contains two non-contact electrodes, both the size of the electrodes

and the space between the electrodes have great influences on the performance of the sensor. The ground plane also plays an important role. Because the parasitic capacitance of the sensor is related to the electric field's (e-field) path to ground, it is important to choose a ground plane that limits the concentration of e-field lines with no conductive object present[204]. Because of its property, capacitive sensor is mainly used in the application of touch screens[205]. Usually Capacitive sensor dimensional measurement requires three basic components: a probe that uses changes in capacitance to sense changes in distance to the target, driver electronics to convert these changes in capacitance into voltage changes, and a device to indicate and/or record the resulting voltage changes[206]. In most cases, textile based capacitive sensors are made by laying different functional layers together. As shown in the Figure 8 below, during the manufacturing process for the electrodes a simple textile pattern of alternating conductive and isolating strips, while the routing is achieved by soldering wires connecting each electrode strip with the printed circuit board(PCB) for the readout. The wires were bundled together and stuck to the fabric. Since the routing is achieved by wires the area overhead of the routing should become almost negligible, since the wire can be bundled to occupy less area. Finally tow isolated fabrics were added to opposite side of the foam layer[207]. There are several evidences about capacitive sensors used in textile. It was reported in González-Sánchez's work that this sensor can be used to detect breathing and heart signals[208].

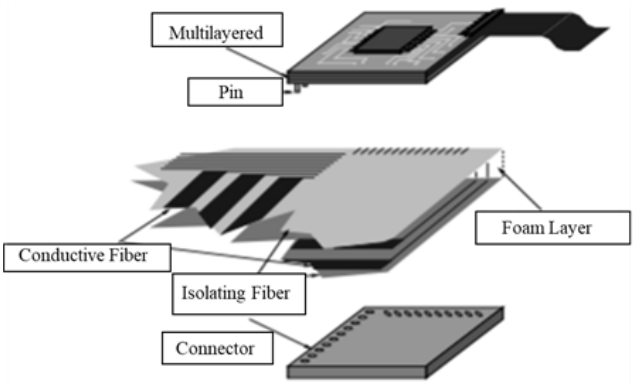

Figure 8. Structure of capacitive sensor[207]

In Se Dong Min's research[209], a single channel capacitive proximity pressure sensor and gait monitoring system for smart healthcare was produced. However, capacitive sensor also shows some disadvantages, one of which is that it is too sensible to changes in environmental conditions such as temperature and humidity. Furthermore, the measurement of capacitance is hard compare to measurement of resistance and the results are usually non-linearity[210]. As this research aimed to produced textile-based pressure sensor, those are problems that will significantly influence the accuracy of measurement during this research.

2.4.3 Piezo-resistive sensors

Piezo-resistive sensor is designed based on the principle of piezo-resistive effect. Piezo-resistive effect was first found in 1856. It was reported that the electrical resistance changed as the mechanical force was applied on the sensor [211]. In conducting and semi-conducting materials, while their bandgaps are affected by the force (like strain) applied on them, the inter-atomic spacing would be changed as well. When the inter-atomic spacing is smaller than before, it is easier for the electrons to be raised into the conduction band, so that the electrical resistance of the material changes. In

homogeneous structure, the electrical resistance (R) is influenced by its dimension and resistivity. The force applied on the material usually causes the change in dimension, thus change the electrical resistance. The electrical resistance can be calculated using resistance equation derived from Ohm's law:

$$R = \rho \frac{L}{A} \tag{2-1}$$

where,

ρ = resistivity

L = length

A = cross-section area of the current flow[212].

Several evidences can be found from literature, piezo-resistive effect is widely used in the production of textile sensors. In Ozgur Atalay's paper[213], yarns were knitted in the way that they intermeshed with each other. To construct the intermeshed conductive zones, polyester-bended yarns with 20% (weight ratio) stainless steel fibres and silver-coated nylon were used as the sewing thread within non-conductive base structure. The nonconductive base structure was made of polyester yarn and 800-dtex double covered Lycra yarn. They also created a second design of the sensor. In this design[213], conductive yarns were knitted into a base structure in a series of conductive courses. The courses were separated from each other by non-conductive courses. At the beginning, the conductive courses were knitted into an elastomeric single jersey structure. The basic structures were interlock structures with a series of conductive courses in plain loop arrangement. It has also been confirmed that the piezo-resistive works well as compression sensor. In Lai's research[214], the production of

compression sensor was carried out. The sensor was designed to be a three-layer piezo-resistive sensor. The middle layer of the fabric consisted of a piezo-resistive plastic sheet (Velostat) and it was sandwiched between two conducting layers. The conducting layers acted as electrodes, they consisted of either conducting fabric or conducting thread. While pressure force applied on the fabric sensor, the resistance of the piezo-resistive Velostat would change so that the compression force could be measured. The conducting fabric was made from medical grade elastic fibre which was 76% Ag plated and 24% Nylon. Duct tape was used as a general adhesive and package[214].

Figure 9. Lai's piezo-resistive sensor[214]

It can also be found that piezo-resistive based pressure sensor can be used to measure both strong and weak pressure signals. In Hamdani's research, piezo-resistive pressure senor was designed to measure cardiorespiratory signal, the sensor was designed into three layers as well[215]. There are also evidences showed that piezo-resistive pressure can be used to make sensor matrix to measure at large area. In Ilaria Baldoli's article, the sensors were assembled in a multilayer (or sandwich) matrix structure (Figure 10). The piezo-resistive textile used was a stretchable and knitted fabric which composed of 91% of Nylon and 9% of elastane. The fibres within the fabric were coated with conductive polymer, so that they could provide both superficial and transversal electrical resistance (respectively 30–50 kΩ/100 mm and ~0.05 MΩ through the 0.5mm

thickness). The electrical resistance tend to decrease as stretch and pressure force applied. The middle layer was the resistive sheet, and it was sandwiched by two layers that consisted of a non-conductive textile. Several conductive stripes which were parallel to each other (20mm wide) were in the non-conductive textile. The strips were obtained by sewing multiple copper threads (with a diameter of 110μm), in this way a pattern of alternate conductive and insulating bands was created. The outside layers with the thickness of 0.65mm were cut from pre-manufactured fabric. They were placed in a way that the conductive stripes on the top and the bottom layer were orthogonal to each other and to create a grid. The crossing of row with column produced the pressure sensitive element. After all the three layers were prepared, they were held together with stitches, which did not change the electrical properties of the fabrics. Then additional outer layers of felt were applied to protect the wear and tear. The overall thickness of the sensor was around 4.6mm. The sensor matrix included 8 rows and 8 columns with a total of 64 sensors[216].

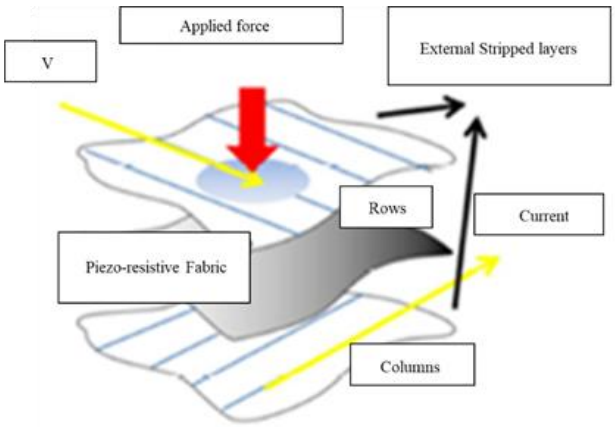

Figure 10. Piezo-resistive sensor matrix[216]

In summary, piezo-resistive effect based sensors are highly valued for their high sensitivity and linearity[217][218], which made them suitable for the textile-based

pressure senor in this research. Their high sensitivity and linearity could help to produce more accurate results during this research.

2.5 Summary

In this chapter, previous research on coffee ring effect, components of electro-conductive inks, substrate and working principle for textile-based sensors as well as impregnation methods were critically reviewed based on the aim and objectives of this research.

The literature review revealed the following gaps for the research area in concern:

1. The coffee ring effect is undesired for the end uses of the water-based inks. How to avoid coffee ring effect on fine nonwoven polyester substrate is still a hot topic of research for the development of water-based inks.
2. The optimal parameters, in terms of particle size, viscosity and surface tension for water-based carbon ink to be coated on fine nonwoven polyester fabrics for pressure sensors are still not fully studied and presented.
3. The information based on previous experiments is not enough to reveal the influences of the carbon particle distribution and carbon take-up rate on the performance of the nonwoven polyester based pressure sensor, which is critical important for the development of textile-based sensor.

Chapter 3 Development of carbon ink

Electro-conductive ink plays the key role in the development of wearable sensors. The challenge in this research is to produce a type of water-based carbon ink which is free from coffee ring effect. The ink should also have suitable particles size, viscosity and surface tension for the coating of fine nonwoven polyester based pressure sensors.

3.1 Components of the carbon ink

Electro-conductive inks should contain solvent, functional particles, binders and additives. Based on the purpose of developing a coffee ring effect free ink, the components of the ink were selected. Water was chosen as main solvent and polyethylene glycol was used as co-solvent. Guar gum was used as viscosity modifier and xanthen gum was chosen to be the binder. Triton X-100 was chosen as surfactant and stabliser.

3.1.1 Solvent and co-solvent

1) Solvent

Solvent is the diluent to the other ink components. The main function of solvent is to keep the ink in a form of liquid during the coating/printing process before it is finally deposited onto the substrate. Traditional, inks produced for textile are polyvinyl chloride based chemical solvents, which are toxic and expensive. In this research, water was used as the solvent because it is a non-toxic environmental friendly solvent. Water is cheap and easy to achieve. Furthermore, no harmful solvents are required for the cleaning of water-based ink after coating/printing. The boiling point of water is 100℃ under standard atmospheric pressure, which leads to a short drying time. Additives

would be added to make the water-based ink suitable for dip coating.

2) Co-solvent

Polyethylene glycol was used as co-solvent to make up for some of solvent disadvantages. The first function of co-solvent was to avoid the coffee ring effect which can be commonly seen among water-based inks. The coffee ring effect would lead to the carbon particles aggregated to the edges of an ink drop during drying. This would lead to nonuniform distribution of the carbon particles on the substrate. In order to avoid the coffee ring effect, polyethylene glycol was used in this research. The hypothesis was that the different properties of water and polyethylene glycol would lead to a gradient to create an inner flow during drying process and balance the outward flow to avoid the coffee ring effect. The second function of co-solvent was to increase the viscosity of the ink. The polyethylene glycol used in this research was P3015-polyethylene glycol (Sigma-Aldrich) with average mol weight of 200. The liner formula of it is (C2H4O)nH2O. With an average mol weight of 200, this type of polyethylene glycol was clear colorless liquid. The Brookfield viscosity of this polyethylene glycol was 43-57 mPa.s. It is non-toxic, non-irritant, slightly bitter, water-soluble, and has good solubility with many organic components. It was added to deionized water with a ratio of 1: 10 polyethylene glycol and water by mass.

3.1.2 Carbon particles

Carbon particles have longer lifetime than metal particles. They have already been widely accepted as a type of cheap and easy-making material for conductive ink. However, the challenge is how to control the carbon particle size within the ink. During

the dispersion process carbon particles could aggregate and form larger carbon particles, those large particles could block the pore between fibres and influence the coating process. However, there are no researches determined how small conductive particles should be according to different pore sizes. Because of this, the size of the carbon particles after dispersion should be studied. In this research, it was tried to achieve the smallest size of carbon particles to form a uniform coating. Activated carbon was used as the electro-conductive particles in this research. The activated carbon particles used in this research is 633100-carbon (Sigma-Aldrich) which is a type of activated charcoal powder. Water bath ultra-sonicator would be used to study how to adapt the carbon particle size within the ink.

3.1.3 Binder and viscosity modifier

1) Binder

The function of binder is to provide adhesion of the carbon particles to the substrate. In this research xanthan gum was used as the binder. Xanthan gum (xanthan gum), is a type of microbial extracellular polysaccharide produced from Xanthomonas campestris through fermentation engineering with carbohydrate as the main raw material (such as corn starch)[219][220]. It has unique rheology, good water solubility, stability to heat and acid and alkali, and good compatibility with a variety of salts. As shown in the Figure 11 below, it is an anionic polysaccharide composed of a β-(1→4)-D-glucopyranose glucan backbone with side chains of (1→3)-α-D-mannopyranose-(2→1)-β-D-glucuronic acid-(4→1)-β-D-mannopyranose on alternating residues.

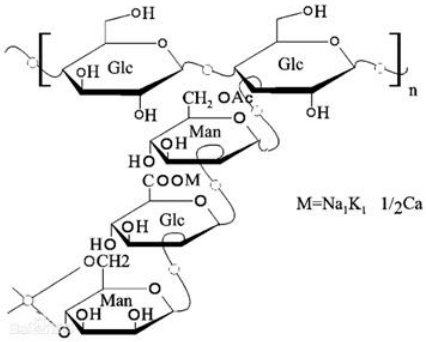

Figure 11. Chemical structure of xanthan gum[227]

The xanthan gum used in this research was "G1253 Xanthan gum from Xanthomonas campestris" (Sigma-Aldrich). The xanthan gum is in a form of powder with faint yellow appearance. It is harmless and is widely used in the food and medical industry. It was selected as binder to allow the retention of the electrical properties of the ink. The major advantage of xanthan gum over other binders is its biocompatibility. Another advantage of xanthan gum is that it can increase the viscosity of the ink. Xanthan gum can dissolve rapidly in water and has good water solubility. It can also be dissolved even in cold water, which makes it possible to leave out the complex processing process. It shows good stability against pH (around 2.5-11) and heat (10-80℃).

2) Viscosity modifier

The function of viscosity modifier is to adapt the viscosity of the ink. The challenge in this research is that the viscosity of water is too low (only 1 mPa.s), thus the viscosity of the ink should be increased to be suitable for printing/coating. The viscosity modifier used in this research was guar gum. Guar gum (also known as guaran) is a galactomannan polysaccharide extracted from guar beans and is always produced as a as a free-flowing powder.[221]

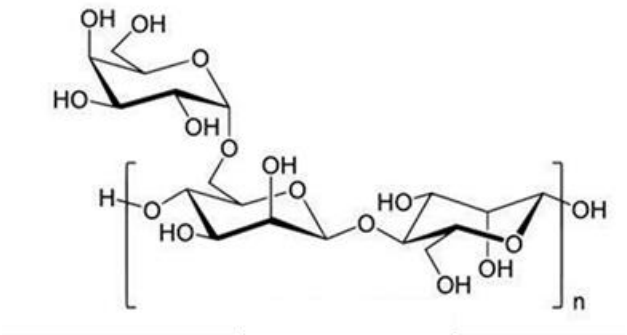

Figure 12. Chemical of guar gum[228]

Chemically, guar gum is an exo-polysaccharide composed of the sugars galactose and mannose. Guar gum has its advantages as viscosity modifier, because of the extra galactose branch points it is more soluble than locust bean gum. It is nonionic and hydrocolloidal in water and will not be affected by the ionic strength or pH. Due to its high ability to flow and deform, it can influence the viscosity of solvents and is widely used as a thickening agent in foods and medicines for humans and animals. It has been found that while guar gum and xanthan gum were added between a ratio of 9:1 and 3:7, synergistic rheological effects occurs. The guar gum used in this research was "G4129 Guar" (Sigma-Aldrich). It was in the form of powder with yellow colour.

3.1.4 Surfactant

The function of surfactant added in electro-conductive ink is to adapt the surface tension and stabilize the conductive particles within the ink. The challenge in this research is that the surface tension of water is too high (73 mN/m), thus it should be decreased. Another challenge is how to stabilize the carbon particles to achieve a longer shelf life. In this research nonionic surfactant was used. Nonionic surfactant is a type of surfactant whose main hydrophilic group is ether group, which is contained in the molecule and does not dissociate in the aqueous solution. Compared with ionic surfactants, non-ionic

surfactants do not exist in ionic state in solution, thus they have high stability and are not easy to be affected by the presence of strong electrolytes or by the influence of acids and bases. Triton X-100 was chosen to be the suitable nonionic surfactant in this research. Triton X-100 is a common non-ionic surfactant and emulsifier which is often used in biochemical applications to solubilize proteins[222]. It is considered a comparatively mild detergent, non-denaturing, and is reported in numerous references as a routinely added reagent. It has a hydrophilic polyethylene oxide chain and an aromatic hydrocarbon lipophilic or hydrophobic group, and the hydrophobic group is known as a 4-(1,1,3,3-tetramethylbutyl)-phenyl group. Because of the hydrogen bonding of the hydrophilic polyethylene oxide parts, Triton X-100 appears as a clear viscous fluid. It is soluble in water, toluene, xylene, trichloroethylene, ethylene glycol, ethyl ether, ethyl alcohol, isopropyl alcohol, and ethylene dichloride under a temperature of 25°C. The surfactant used in this research was “T9284 Triton X-100” (Sigma-Aldrich). The linear formula of it is t-Oct-C6H4-(OCH2CH2)xOH, where x= 9-10. It has a CMC of 0.2-0.9 mM (20-25°C) and a HLB of 13.5.

3.2 Experiments

In order to produce a water-based carbon ink, the main steps were: mixing of main solvent and co-solvent, carbon particle dispersion, viscosity modification and surface tension modification, the formulation process was done within a fume cupboard as carbon nanoparticles were used.

3.2.1 Dispersion of activated carbon particles

Among all the coating/printing methods, inkjet printing is strict to the particle size

within the ink. According to literature review, the particle size should be 1/50 of the nozzle head to avoid clog of the nozzle head. It was found that for the commonly used Epson 4880c inkjet printer, inks with particles less than 2μm could be printed without nozzle clog. Because of that, the particle size analysis process was done after the dispersion of carbon particles. During the research about particle size, ink with concentration of 5mg/ml was used. The ink was diluted in order to get a clear shape of carbon particles and then dropped on Si/SiO_2 substrate plates. The reason of using Si/SiO_2 is that silicon is opaque and silicon dioxide is transparent, a layer of silicon dioxide should be coated on silicon for convenient observation. Si/SiO_2 substrate plates are commonly used for the observation of inks under optical microscope, SEM and AFM. Ten samples were tested under optical microscopy and 10 positions were picked across each sample. After that statistical analysis of all 100 particles were done. Ultrasound water bath sonicator was used to adapt the carbon particle size within the ink. During the ultra-sonication process, carbon ink was put into a glass bottle and then put into a tank full of water. During the ultra-sonication process, under the effect of ultrasound waves, localized bubbles (commonly termed as 'cavitation') were generated in the liquid. The bubbles then collapsed and generated high shear forces to break the large carbon particles. Ice bags were added into the water to cool down the machine. In order to figure out the relationship between sonication time and the particle size, the ink samples were sonicated for 2h, 4h, 6h and 12h till the machine was overheated (more than 40℃).

3.2.2 Surface tension adjustment

The surfactant in this research have two functions: reducing the surface tension of the ink and stabilizing the carbon particles. Although, it was found that the CMC of the "T9284 Triton X-100" (Sigma-Aldrich) used in this research was 0.2-0.9 mM (20%-25%), a surface tension test was still needed to figure out how the surface tension of the ink changed with different amounts of surfactant added. The pendant drop tests were conducted to measure the surface tension of the ink.

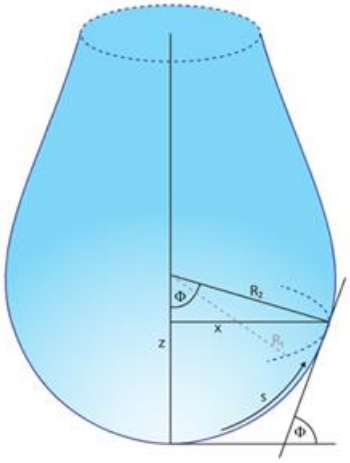

Figure 13. Young-Laplace fit on a pendant drop [108]

The pendant drop method is based on the Young-Laplace equation. The equation below demonstrates the Laplace pressure between the areas inside and outside of a curved liquid surface/interface (△P) with the principal radii of curvature R_i:

$$\Delta P = P_{\text{int}} - P_{ext} = \sigma \left(\frac{1}{R_1} + \frac{1}{R_2} \right) \quad (3\text{-}1)$$

Two forces determine the shape of the drop: surface tension and gravitation. The surface tension tends to minimize the surface area and get the drop into a spherical shape. Gravitation on the other hand stretches the drop from this spherical shape and the typical pear-like shape results.

Figure 13 shows an image of a typical pendant drop. Based on Pascal's law a pressure difference is caused across the z-axis by gravitation. Therefore the Laplace pressure ΔP (z) at a distance z from an arbitrary reference plane with Laplace pressure ΔP_0 is:

$$\Delta P\ (z) = \Delta P_0 \pm \Delta\rho gz \tag{3-2}$$

For a pendant drop the principal radii of curvature at the vertex (lowest point of the drop) are: $R_1=R_2=R$. Thus it is convenient to place the reference plane in this point. For every point above it holds $R_2=x/\sin\Phi$. The mentioned equations lead to:

$$\frac{1}{R} + \frac{\sin\phi}{X} = \frac{2}{R} \pm \frac{\Delta\rho gz}{\sigma} \tag{3-3}$$

where, R is the principal radii of the curvature at the vertex and △ρgz is a hydrostatic pressure.

The introduction of a parametrisation using the arc length of the drop shape results in the following set of three first-order differential equations with three boundary values, which is solvable by numerical procedures:

$$\frac{d\phi}{ds} = -\frac{\sin\phi}{x} + \frac{2}{R} \pm \frac{\Delta\rho gz}{\sigma} \tag{3-4}$$

$$\frac{d\phi}{ds} = \cos\phi \quad ; \quad \frac{dz}{ds} = \sin\phi$$

$$0 = x(s=0) = z(s=0) = \phi(s=0)$$

The numerical fit of the theoretical drop shape to the shape recorded by the camera eventually yields the surface tension. The described considerations also apply when the surrounding phase is not air but another liquid. In this case the interfacial tension is evaluated. Although the principal and formula used to calculate the surface tension of a pendant drop is complex, with the help of modern goniometer and the software

supplied, computers can automatically derive the surface tension of any liquid, thus the complex computation process of the users are no longer needed.

Figure 14. DSA Drop Shape Analysis System (Krüss)

In this research, the DSA Drop Shape Analysis System (Krüss) was used to measure the surface tension of the ink. During the test progress, a drop was suspended from a needle, and then the image was captured by the camera. Then the image is analyzed with the help of the DSA software, based on the shape of the drop and the Young-Laplace equation, the surface tension of the ink was measured. During the ink formulation process, ten different amounts of surfactant (from 0.02 mg/ml to 0.2 mg/ml) were added to figure out how the surface tension of the ink change with the amounts of surfactant added. In order to figure out if the amount of viscosity modifier added would influence the surface tension of the ink, further tests should be conducted. For samples with different concentrations of surfactant, 5 different amounts of viscosity modifier were added (0.05 mg/ml, 0.1 mg/ml, 0.15 mg/ml, 0.2 mg/ml and 0.25 mg/ml). The surface tension of all these samples were tested and plotted.

3.2.3 Wettability tests

Inks should have good wettability for coating/printing. In order to figure out the wettability of this ink, contact angle test was carried out. If the contact angle is smaller than 90°, the solid surface is considered hydrophilic to the liquid. If the contact angle is bigger than 90°, the solid surface is considered hydrophobic. If the contact angle is 0°, the phenomenon is called ideal spreading, which means the liquid molecules are strongly attracted to the solid molecules and a 100% wetting is achieved. The method used to measure contact angle was based on the Young–Dupré equation. Based on the theory, contact angle is caused by the thermodynamic equilibrium between the three phases: the solid phase (s), the ink (i) and the vapour (v). Based on the Figure 15, solid–vapor interfacial tension is represented by $\gamma_{s\text{-}v}$, the solid–ink interfacial tension is represented by $\gamma_{s\text{-}i}$, the ink–vapour interfacial tension is represented by $\gamma_{i\text{-}v}$, and the contact angle is represented by θ. Based on the Young's equation, the angle θ can be calculated as:

$$\cos\theta = \frac{\gamma_{s-v} - \gamma_{s-i}}{\gamma_{i-v}} \tag{3-5}$$

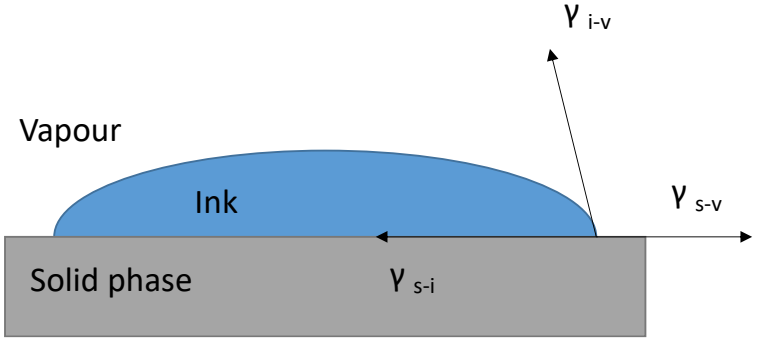

Figure 15. Principle of contact angle test

In this research the sessile drop test was done with the help of DSA Drop Shape

Analysis System (Krüss). Ink with no surfactant added was first tested. The drop was dropped on glass plate which was commonly used for this experiment.

3.2.4 Viscosity adjustment

Viscosity is one of the important parameters in ink formulation. All inks should have the viscosity appropriate to the coating/printing process. Viscosity of ink is determined by shear, shear stress as well as the shear rate (under an applied shear stress). During the coating/printing process, the ink flows, which can be considered as a cube of flow which has a velocity gradient based on its flow rate and is known as shear rate (s^{-1}). Table 1 shows that different coating/printing processes have different ranges of viscosity that suit them.

Table 1. Viscosity of inks for different coating/printing methods [223]

Coating/printing methods	Viscosity (mPa.s)	Shear rate (s^{-1})
Dip coating	50-1000	10-500
Ink-jet printing	4-30	10-5000
Screen printing	1000-10000	1-1000
Gravure printing	100-1000	10-1000
Flexographic printing	1000-2000	10-1000

The viscosity of water is 1mPa.s which is not suitable for any of the methods in this table, viscosity modification is required. In this research, two types of viscosity modifier were added: xanthan gum and guar gum. Xanthan gum also worked as binder for its biocompatibility. The two gums were added together (1:1) to increase the viscosity of ink. 0.05 mg/ml, 0.1 mg/ml, 0.15 mg/ml, 0.2 mg/ml and 0.5 mg/ml were added into the ink to figure out how much the viscosity of the ink can be increased.

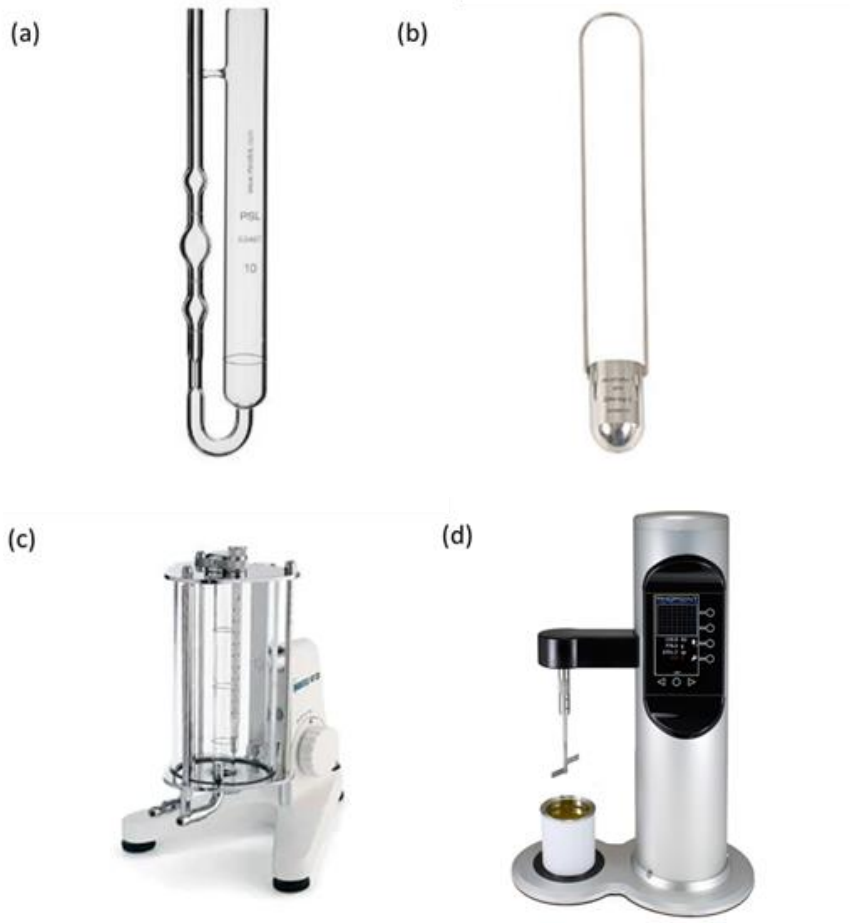

Figure 16. (a) Apillary Viscometer (b) Zahn Cup (c) Falling Sphere Viscometer (d) Vibrational Viscometer

Viscometer was used to measure the viscosity of the ink. Although several viscometers can be used to test the viscosity of a conductive ink as Apillary Viscometer, Zahn Cup, Falling Sphere Viscometer, Vibrational Viscometer and Rotational Viscometer[224]. Apillary Viscometer is a very early used instrument to measure viscosity. In this instrument, capillary tubes are used. By measuring the time it took for a volume of liquid to pass through the length of the tube the viscosity of the fluid can be measured. The Zahn Cup method is similar to the previous one, during the measuring process, a small container with a handle and a small hole in the bottom is used. To measure the time it takes to empty the cup through the hole, the viscosity can be calculated. In the

Falling Sphere Viscometer, a sphere of known density is dropped into the fluid sample. By measuring and recording the time it takes for the sphere to fall to a specified point, the viscosity can be calculated. This method is now mainly used on ships to monitor the quality of the fuel going into the ship's engine. Vibrational Viscometers measure the damping of an oscillating electromechanical resonator immersed in a fluid. This technique is often used in-process to give continuous readings in a product stream, batch vessel, or in other process applications. Rotational viscometer measures the torque required to turn an object in a fluid as a function of that fluid's viscosity. This method is frequently used in quality control and production laboratories.

Figure 17. Plate-to-plate viscometer

In this research, one of the rotational viscometer known as plate-to-plate viscometer was used because it can apply different shear rates to the liquid. During the test, while the machine was calibrated, the fluids to be tested were pulled on the bottom plate. The amount of fluid should be controlled to a suitable amount for the test accuracy. The distance between two plates was set to be 600nm. The test was done at controlled room temperature (25℃) with an increased shear rate from 10 (1/s) to 500 (1/s). The shear

rate of the viscometer could not be higher, as a higher shear rate could lead to overheating of the machine and the machine would stop by itself. In order to figure out if the surfactant added would influence the viscosity of the ink, all the combinations with different amounts of viscosity modifier and surfactant added were tested. Finally the viscosity would be recorded based on the equation:

$$\eta = \frac{T}{r'} \tag{3-6}$$

where, T is the shear stress and r' is the shear rate.

In order to figure out if the surfactant added would have an influence on the viscosity of the ink, ten different amounts of surfactant (from 0.02 mg/ml to 0.2 mg/ml) were added to the samples with 0.1 mg/ml viscosity modifier added. The viscosities of those samples were measured and the testing results with different amounts of surfactant added were collected and plotted.

3.3 Results and discussion

3.3.1 Effects of sonication time on particle size

Figure 18 shows an image the carbon particles within the ink without any sonication. The ink was diluted so that the shape of the carbon particles can be clearly observed. The size of a total number of 100 carbon particles were measured and plotted into a graph.

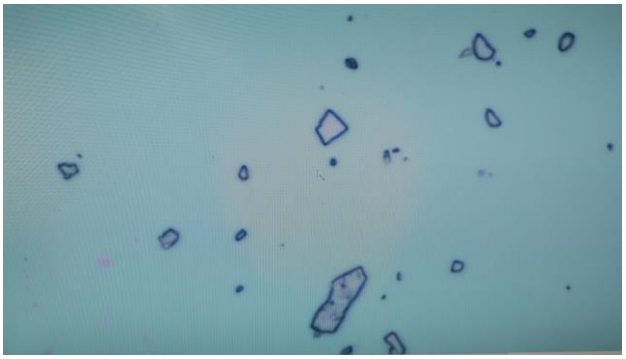

Figure 18. Carbon particles under optical microscope

As can be found from Figure 19, it can be found that the carbon particles aggregated during the dispersion process, about 30％ of the carbon particles were even bigger than 10μm. Based on this result, adaption of the particle size was needed. In this research, the water bath ultra-sonication method was used to adapt the carbon particle size.

According to Figure 19-B, it can be found that after sonication of an hour, the size of the carbon particles had been significantly reduced, about 90％ of the particles are now smaller than 5μm. However, the size of most particles still did not match the required 2μm. Because of that, further ultra-sonication was needed.

Based on Figure 19-c, it can be found that after 2 hours' sonication, 90％ of the carbon particles are now smaller than 2μm, however there are still about 8％ of the particles are between 2 to 2.5μm and some even bigger than 4μm. 2 more hours of ultra-sonication was done to further break down the big particles, during this process ice bags were added to cool down the water temperature to room temperature. Figure 19-D shows that after 4 hours, the particle size was further reduced. The sizes of all the carbon particles within the ink were reduced.

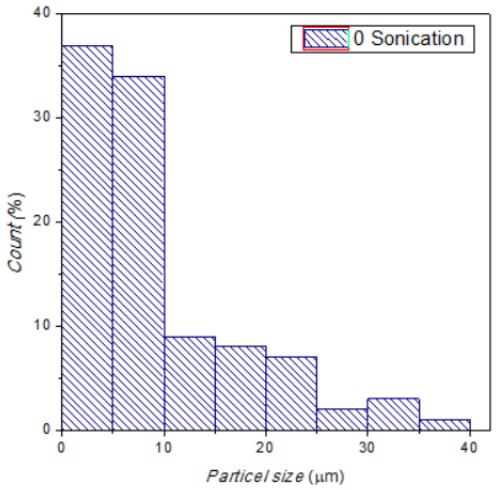

（A）no sonication

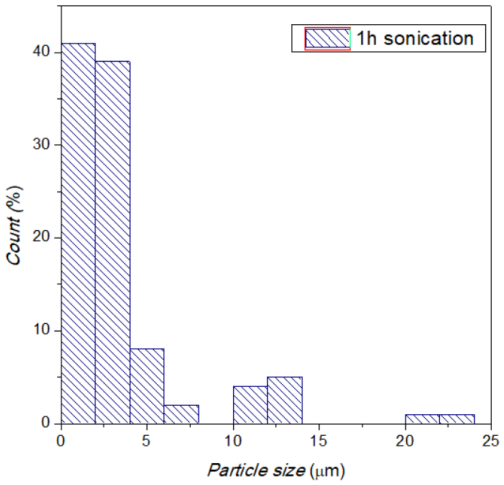

（B）1h sonication

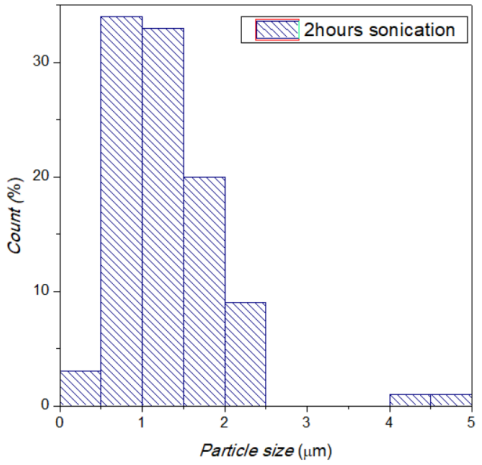

（C）2h sonication

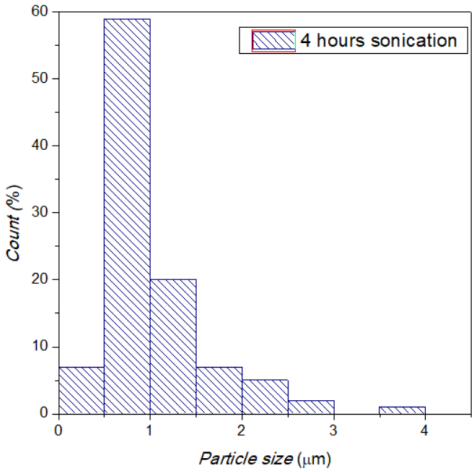

（D）4h sonication

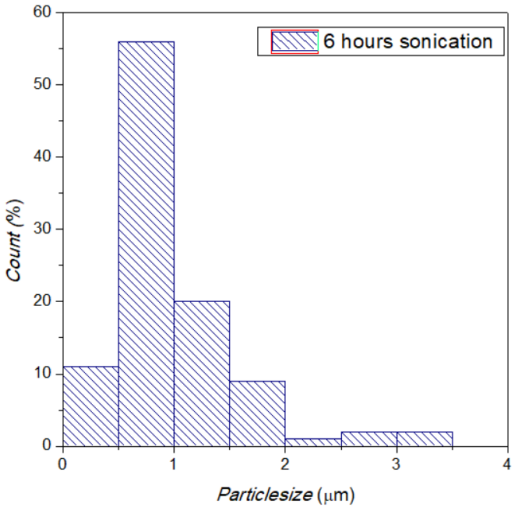

（E）6h sonication

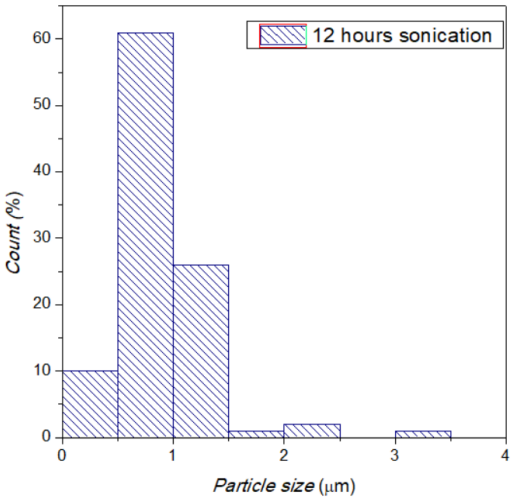

（F）12h sonication

Figure 19. Particle size distribution

Further ultra-sonication was done and it can be found that after 6 hours of sonication more than 90％ of the carbon particles are now smaller than 2μm. In order to figure out the smallest particle size can be achieved for this ink, longer ultra-sonication was carried out. After 12 hours, the water bath ultra-sonicator was overheated (more 40℃) and even the ice bags could not efficiently cool it done, thus the sonication was finally stopped. It can be concluded from Figure 19-F that after sonication for 12 hours, 95％ of the carbon particles were smaller than 2μm. The size of all the particles were further reduced, about 60％ of the particles were between 500nm to 1μm. However, after 12 hours of sonication, even with ice bags used to cool down the water temperature, the water within the tank was still more than 40℃. As high temperature would influence the property of the ink, no further sonication could be down. Thus, the particle size shown in Figure 19-F was the smallest could be achieved in this research.

3.3.2 Effects of surfactant and modifier on surface tension

At the beginning, the surface tension of ink with different concentration of activated carbon added was measure. It was found that the concentration of activated carbon had no influence in the surface tension of the ink. Thus, further tests were based on inks with a carbon concentration of 5 mg/ml. It can be found from Figure 20 that Triton X-100 has a significant effect on the surface tension of the ink. The surface tension of the in without surfactant was about 65 mN/m, with the increasing of the surfactant added, the surface tension sharply decreased and finally reached the lowest point of 32 mN/m. That is because Triton X-100 has hydrophobic tails and uncharged hydrophilic head-groups. While added into the ink, those hydrophilic head-groups can break the lipid-

lipid associations thus lower the surface tension of the ink. It can be concluded that the CMC of Triton X-100 in this ink is 0.1 mg/ml. Although the information from Sigma-Aldrich showed the CMC of Triton X-100 was 0.2-0.9 mM (20%-25%), this test was still necessary. Based on the surface test, the accurate CMC of Triton X-100 for this ink was measured. Furthermore, it shows how the surface tension changes with different amounts of surfactant added. With the help of this graph, it can be easier to control the surface tension of this ink for different applications.

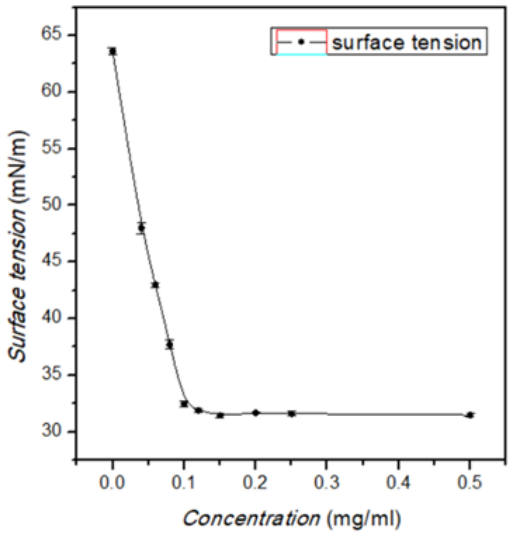

Figure 20. Relationship between surface tension and the amount of surfactant added

(A) (B)

Figure 21. Pendant drop

(A) Without surfactant. (B) With 0.1 mg/ml surfactant

The 3D graph of Figure 22 shows the surfactant of ink with different concentration of

surfactant and viscosity modifier. The purpose of this test is to figure out if different concentrations of viscosity modifier will interact with the surfactant and further affect the surface tension of the ink.

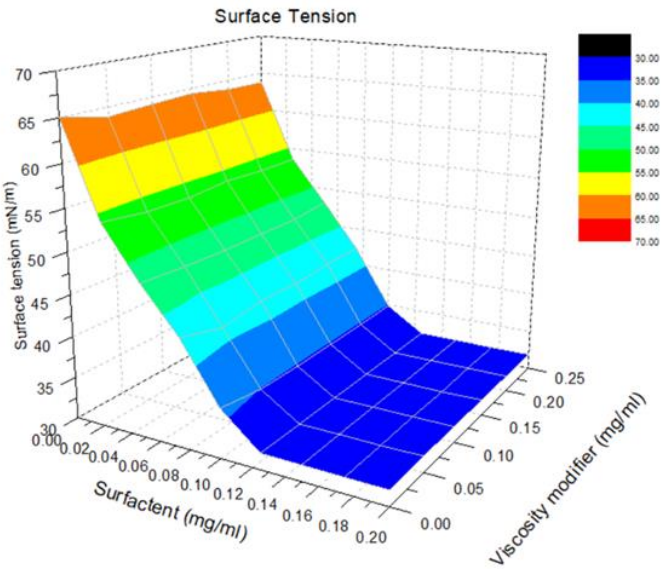

Figure 22. Relationship among surface tension, surfactant and viscosity modifier

The x axis and y axis show the relationship between surface tension and the amount of surfactant added, which is the same as Figure 22. From the y axis and the z axis of the graph, it can be found that the amount of viscosity modifier chosen and added does not have an influence on the surface tension of the ink.

3.3.3 Effects of viscosity modifier and surfactant on viscosity

It can be found from Figure 23 that modifier added significant increases the viscosity of the ink (used to be 1 mPa.s). That is based on the property of the modifier added. When the modifiers dissolve in water, their macromolecular chains are distributed in solvents and intertwined with each other, which increases in the viscosity. At the same time, the interaction between macromolecular chains and solvents (e.g. hydrogen chains with water) makes the whole molecular chain surrounded by solvents. This so-

called hydrodynamic volume increasing and thus the solution viscosity increases. As shown in Figure 23, the viscosity of the ink decreases as the shear rate increases. That is because the co-solvent and viscosity modifier added turned the ink from Newtonian fluid to a type of non-Newtonian fluid with shear thinning effect. The viscosity of the ink decreases quickly with shear rate added, that is because the status of the fluid turns from static to dynamic. Then the viscosity decreases as the shear rate increases and finally goes stable. It can be found from the figure that with 0.05 mg/ml viscosity modifier added, the finally stable viscosity was around 46 mPa.s. When 0.1 mg/ml modifier was added, the viscosity of the ink increased to about 51 mPa.s. The viscosity was 52 mPa.s, while 0.15 mg/ml modifier was added. It was found that with 0.2mg/ml or more modifier added, the viscosity would not increase anymore. The biggest viscosity can be achieved was 55 mPa.s under a shear rate of 500 s^{-1}. It can be concluded that the viscosity of the ink in this research can be controlled between 46 to 800 mPa.s, under a shear rate of 10 to 500 s^{-1}. According to Table 1, the viscosity of the ink was suitable for dip coating.

Based on the purpose of adding as less viscosity modifier as possible, the concentration of 0.1 mg/ml was used to adapt the viscosity of the ink to around 50 mPa.s under a shear rate of 500 s^{-1}.

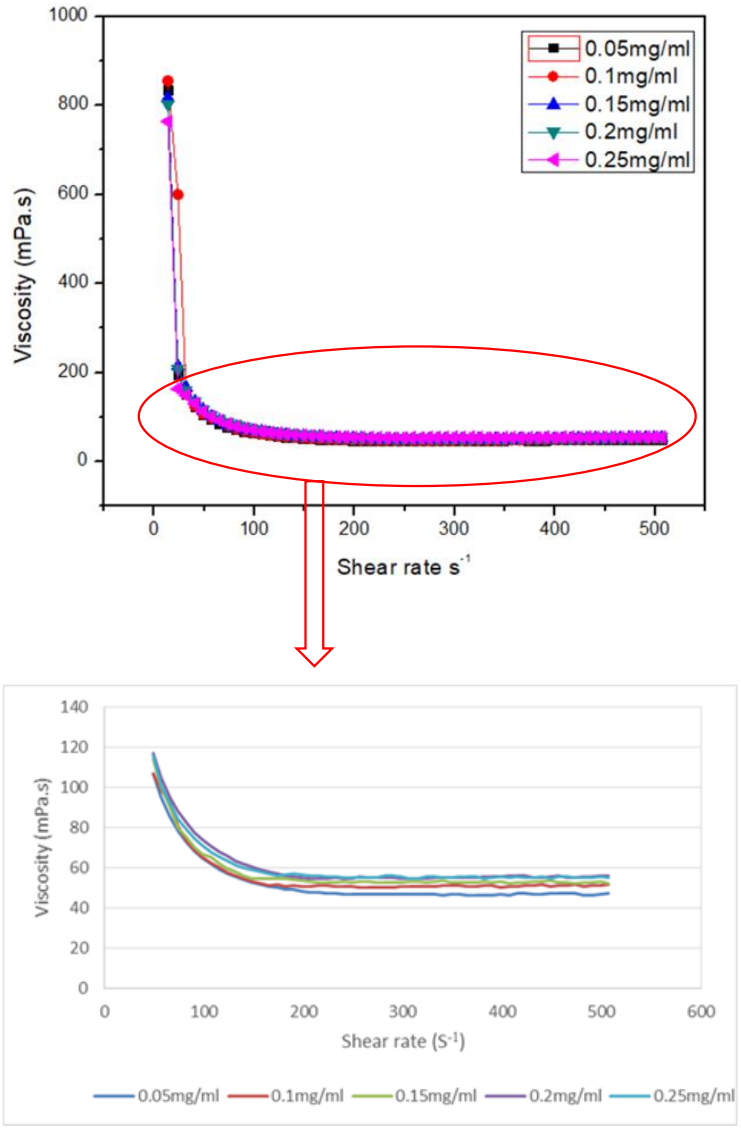

Figure 23. Relationship between viscosity and shear rate with different concentrations of modifier added

However, it was still not sure if different amounts of surfactant added would interact with the viscosity modifier and influence the viscosity of the ink. Samples with different concentrations of surfactant and viscosity modifier were prepared. The viscosity of those samples were measured and plotted into a 3D graph in Figure 24.

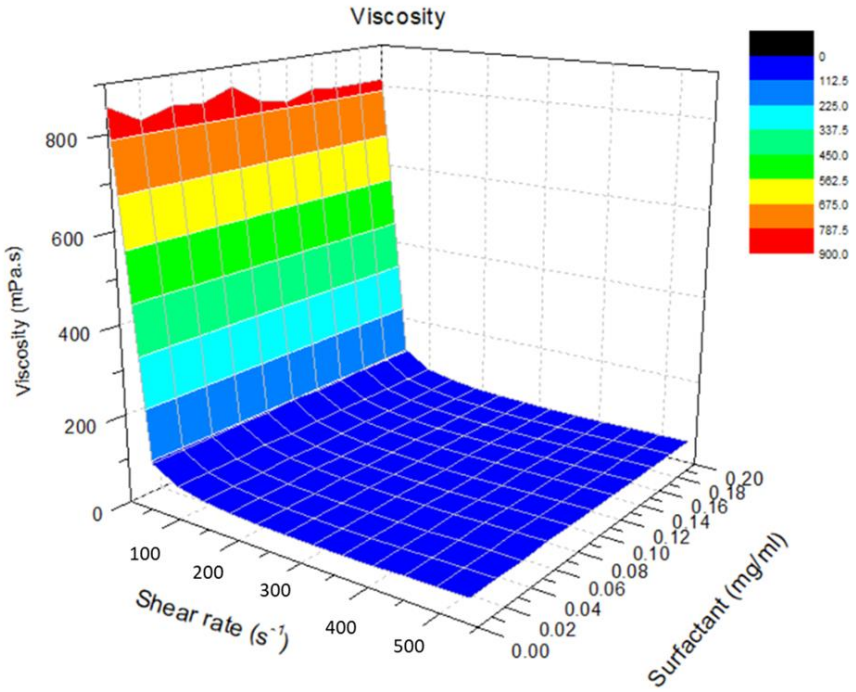

Figure 24. Influence of surfactant on viscosity of the ink

It can be found from Figure 24, that the amounts of surfactant added would not influence the viscosity of the ink, only the amount of viscosity modifier can adapt the viscosity of this ink. Furthermore, this 3D graph can be used as an index for further research, as the viscosity and surface tension under different concentration of viscosity modifier and surfactant was plotted in this graph, any further researches based on this formula can use this graph to pick out the suitable concentration for their purposes without experiments.

3.3.4 Wettability of the ink

According to Figure 25, the contact angle of one drop of the ink on glass plate was already 35° which indicated a good wettability. Because of that, no further improvements on the wettability of the ink were needed.

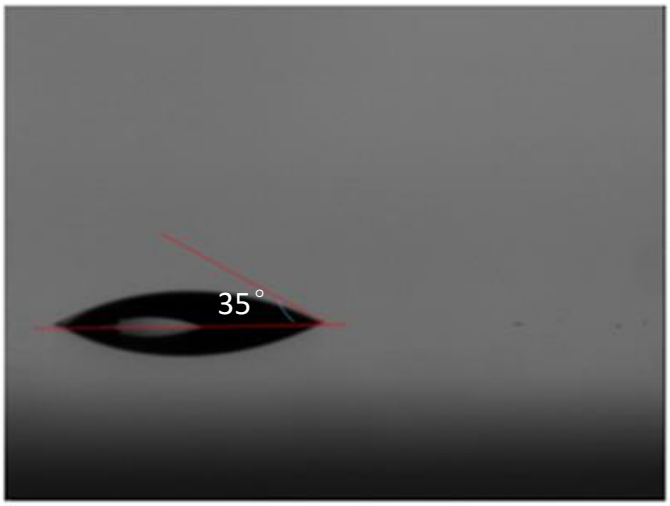

Figure 25. Contact angle

3.4 Summary

The ink developed in this research is based on the following principles:

1) Solvent prepared with a ratio of 1: 10 polyethylene glycol and water by mass.
2) 2, 5, 10, 15, 20, 25, 30 mg/ml activated carbon particles added to the solvent.
3) Water bath ultra-sonication of 2 hours to break down the carbon particles.
4) 0.1 mg/ml (CMC) Triton X-100 added as surfactant to stabilize the carbon partilces.
5) 0.1 mg/ml mixture of guar gum and xanthan gum (1:1) added as viscosity modifier and binder.

The inks with different concentrations of carbon particles were prepared for further coating/printing process. What should be mention is that the use of Triton X-100 as surfactant increased the shelf-life of the ink. The ink can be stored for 15 to 20 days without re-aggregation and sunk of carbon particles based on the concentration of the ink.

Chapter 4 Development of electro-conductive fabrics

In order to confirm if the electro-conductive ink is suitable for the production of wearable sensors, impregnation of fabrics with the ink produced in this research was needed. Based on the electro-conductive fabric samples, their carbon take-up rates and electro-conductivity would be measured. SEM images would be taken to better analyze the distribution of carbon particles.

4.1 Impregnation method and substrate material

Dip coating was finally chosen as the impregnation method used in this research. Because dip coating is a simple and efficient method, furthermore, the range of viscosity can be adapted was most suitable for dip coating. The dip coater used in this research was the Werner Mathis CH-8155 Pad Mangle (Figure 26), which is designed for uniform dyeing, coating, impregnation, and finishing of short fabrics.

Figure 26. Werner Mathis CH-8155 Pad Mangle

Based on previous research [17], it has been proved that fine nonwoven polyester fabric was suitable for the production of textile-based pressure sensor, thus the same type of fabric was used in this research as the substrate. The nonwoven fabrics can be directly made from fibres, the thin fibres make it possible to detect weak signals. Furthermore,

the mechanical properties of nonwoven structure are the same in all directions, which makes it suitable to be the substrate to test the property of the electro-conductive ink. Polyester was chosen as the textile material used for the substrate. The high breaking strength and elastic modulus of polyester make it suitable for wearable sensors. It has been reported that spun-bond nonwoven polyester fabrics have advantages such as high strength, good heat resistance, good stability and breathability. Based on all the advantages above, a type of melt-bond nonwoven polyester fabric was used as the substrate in this research.

4.2 Experiments

4.2.1 Coating of the substrate fabrics

The Werner Mathis CH-8155 Pad Mangle was used for dip coating. In order to make sure the fabric substrates can be fully immersed by the ink, the 150ml of ink were prepared to fully fill the space between the two rollers. During the coating process, inks with different concentrations of carbon particles were used. The following steps were carried out to produce the electro-conductive fabric materials:

1) The fabric was measured and cut into 100mm by 100mm square.
2) The cut fabric was put into the ink and the Werner Mathis CH-8155 Pad Mangle was turned on with a pressure of 2 bar and a speed of 2 m/min. In this progress the rollers led the fabric into the ink solution and then picked it up. The rotate of the two rollers can also shake the solution to achieve a uniform impregnation. The fabric was coated for 30 minutes in room temperature.
3) After the coating process, the fabric was removed and put into the oven for drying.

The temperature of the oven was set to be 100℃ and the fabric was dried for 30 minutes.

4) The dried 100mm by 100mm fabric was then cut into four 50mm by 50mm pieces for later usage. As the four pieces were coated in the same process, they can be considered as identical in the carbon concentration. The pieces of coated fabrics will be used to create wearable sensors.

4.2.2 Measurement of the carbon take-up rates

The differences of the appearance of the fabrics before and after coating were quite obvious. The colour of the raw material was white, after coated by inks with a concentration of 2 mg/ml, the colour of it was white/grey. With the ink of 5 mg/ml used, the colour of the fabric turned into black. The higher the concentration used, the darker the colour of substrate fabrics became. The amount of carbon particles attached to the fabric can be quantified using the take-up rate:

$$R_{Take-up} = \frac{W_1 - W_0}{W_0} \times 100\% \quad (4\text{-}1)$$

where, W_0 is the weight of substrate fabric before impregnation, W_1 is the weight of the dried fabric coated with carbon ink.

4.2.3 Measurement of electro-conductivity and microscopy analysis

The electro-conductivity of the samples was tested using multimeter to figure out the relationship between take-up rates and electro-conductivity of the coated samples.

To further analyze how the carbon tale-up rate influences the electro-conductivity of the coated fabrics, all the samples were put under SEM. SEM images were taken to analyze the structure of the coated fabrics.

4.3 Results and discussion

4.3.1 Relationship between take-up rate and electro-conductivity of the samples

Table 2 shows the take-up rates of different samples coated by inks with different concentration of carbon particles. All the samples were coated by the same coating machine and the coating time were also the same. It can be found that the higher concentration used, the higher carbon take-up rates could be achieved. It is also found that samples with a higher take-up rate have lower electro-resistance. The sample coated with ink concentration of 2 mg/ml showed no electro-conductivity during the test. The coated samples showed a grey and white colour, thus a possible reason was that the samples were not fully coated under this concentration, the uncoated fibres led to the breakage of the electro-conductive path within the fabric and finally made the fabric nonconductive. In order to verify the correction of this possible reason, fabric samples were put under SEM for further study of their coated structure.

Table 2. Take-up rates of fabrics coated with different concentrations of inks

Samples	Concentration (mg/ml)	Take-up rate (%)	Electro-resistance (Ω)
A	2	43.6	N/A
B	5	70.6	1817
C	10	77.9	1623
D	15	80.2	1478
E	20	84.3	1224
F	25	89.6	946
G	30	92.1	850

4.3.2 Relationship between take-up rate and carbon particles distribution

As can be seen from Table 2, the electro-resistance of sample A coated with ink with concentration of 2mg/ml gone beyond the limitation of the multi-meter (2mΩ) and could not be read. It was considered that this sample was not electro-conductive. To figure out the reason for this, SEM images of all the samples were analysed.

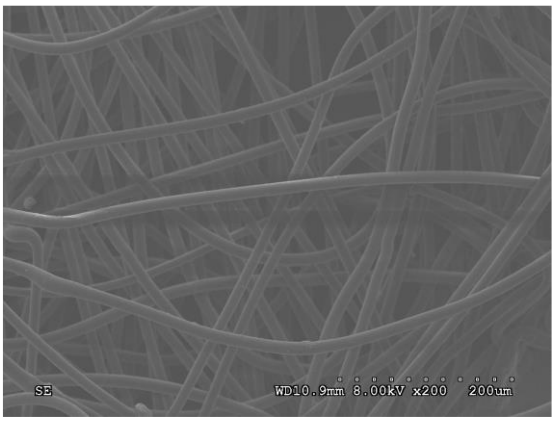

(A) Uncoated nonwoven fabric

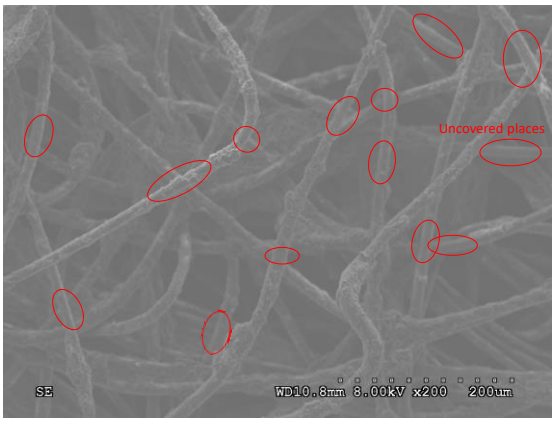

(B) Sample A

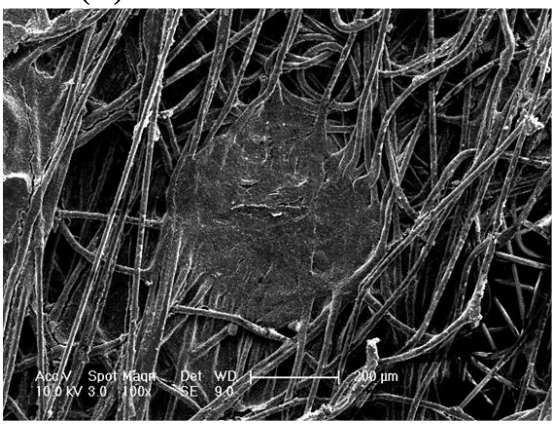

(C) Sample B

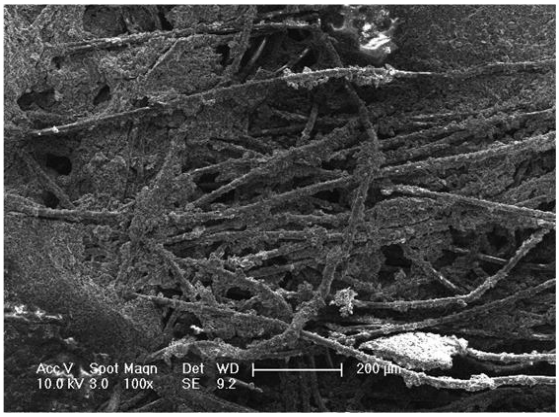

(D) Sample C

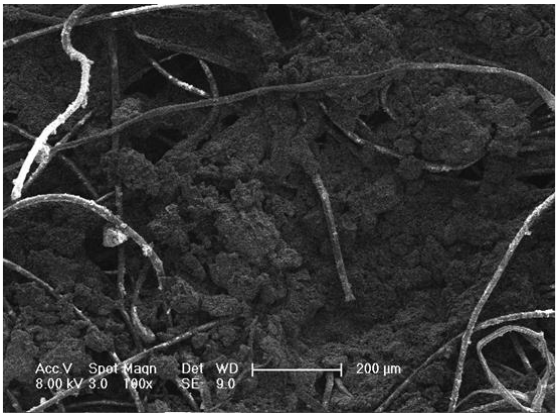

(E) Sample E

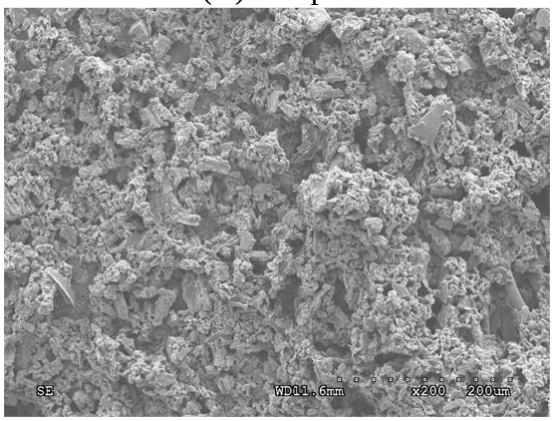

(F) Sample G

Figure 27. SEM images of different samples

Figure 27-(A) shows an image of the uncoated nonwoven fabric. Comparing all the five images shown in Figure 27, it can be clearly seen that after coating, carbon particles covered the fibres within the nonwoven fabric. The carbon particles covered the fibres and made them electro-conductive. The electro-conductive fibres created several eletro-conductive path within the nonwoven structure and finally made the fabric conductive. According to Figure 27-(A) and Figure 27-(B) it can be found that carbon particles were coated onto the fibres within sample A, but they did not fully cover the fibres. The uncovered parts are marked with red circles on Figure 27-(B).

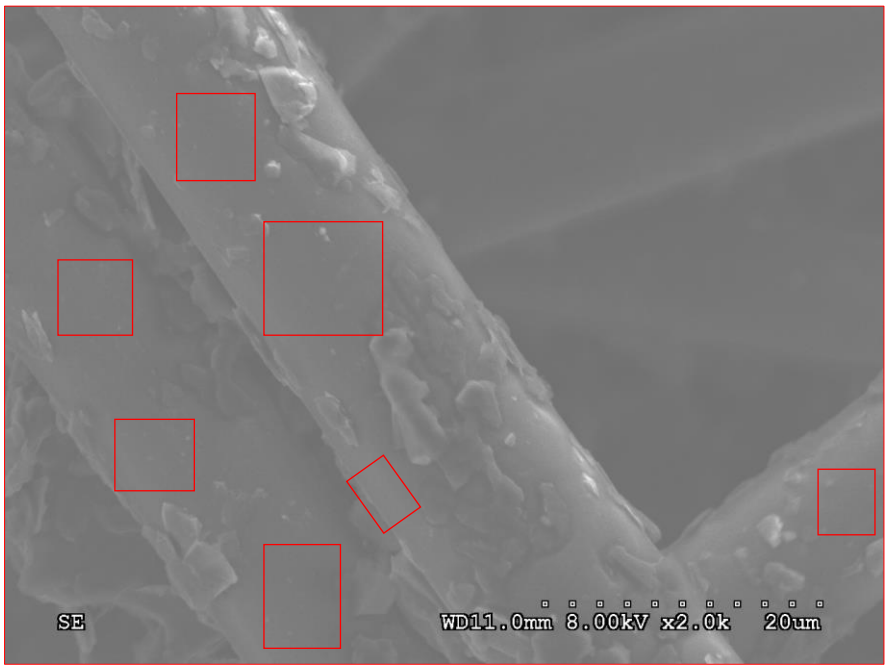

Figure 28. Sample A with magnification x2000

In order to have a clear view of sample A, a SEM image with magnification x2000 was taken. From Figure 28, it can be found that with a low concentration, the carbon particles within the ink could not totally cover the fibres' surface, there are many parts (highlighted with red rectangles) which were not covered by carbon particles. In this case, the conductive particles on the fibre surface were not connected, thus the fibres

could not be electro-conductive and finally led to the non-conductivity of the fabric. The electro-conductive fibres with the coated fabric created many paths for electrons to move and made the fabric electro-conductive. It was also found that with a higher carbon take-up rate, the coated fabrics showed better electro-conductivity. Comparing Figure 27- (C), (D), (E) and (F), it can be seen that there are many spaces between fibres, in Figure 27- (C) the carbon particles just covered the fibres and still left many rooms between fibres. With increasing of carbon take-up rates, more and more carbon particles were coated onto the fibres, the carbon particles gradually gathered and filled the spaces between fibres. Because of this, more and more electro-conductive paths were created for electrons to move and this lead to a lower electro-resistance.

4.4 Summary

It was found that sample A was non-conductive, furthermore, fabrics with higher carbon rake-up rates showed better electro-conductivity. With the help of SEM images the reasons were found.

Chapter 5 Performance Evaluation of ink on wearable pressure sensor

In order to evaluate the properties of the electro-conductive ink in terms of conductivity, sensitivity and reliability, coated fabrics were used to make wearable pressure sensors. The working principle of the wearable sensor was based on the piezo-resistive effect.

5.1 Design and manufacture of the wearable pressure sensor

The wearable sensor was designed as sandwich structure. The complete design and fabrication of the piezo-resistive sensor is illustrated into details based on the images below:

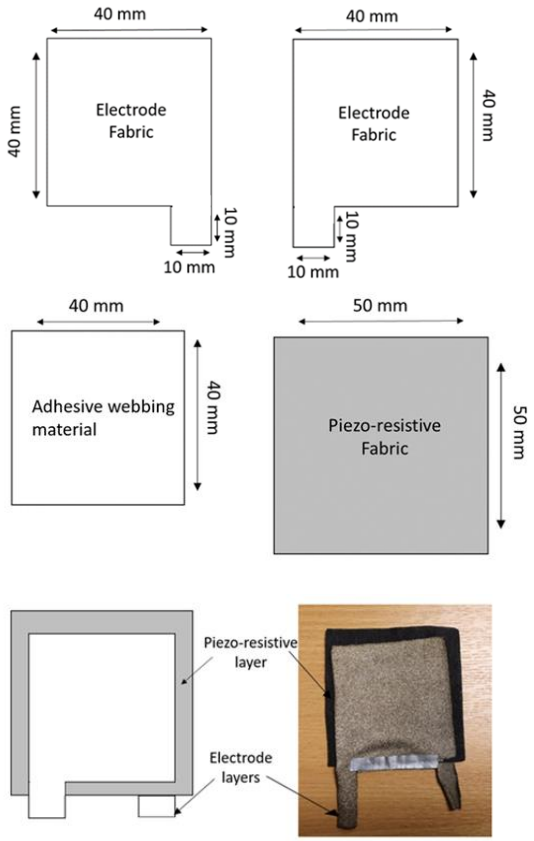

Figure 29. Design of the wearable pressure sensor

As shown in the Figure 29, the sensor consists of five layers. The carbon coated layer

is located in the middle, two silver coated nylon layers are used as electrodes on top and bottom surfaces, and two adhesive layers bond the top and bottom layers with the middle one. The adhesive webbing fabrics were also coated with the carbon inks, because of the low melting point of them (60℃), the adhesive fabrics were dried at the temperature of 45 ℃ for 1 hour. All the five layers were properly aligned and then a steam iron was used to apply a heat of 70℃ for 30 seconds. The webbing materials melt to connect the top and bottom layers to the core layer. The two silver coated fabrics were used as electrodes so that the whole sensor can be connected into Wheatstone half-bridge circuit. In this way the electrical resistance of the sensor along its thickness direction can be measured. The carbon coated layer was designed to be bigger than the electrode layers so that it can avoid the electrical shorting between the top and bottom electrode layers.

5.2 Property measurements

According to the electro-conductive measurement and SEM analysis, sample A showed no electro-conductivity, thus sample A could not be used to produce pressure sensor. Fabrics with higher carbon take-up rates showed better electro-conductivity. However, based on the SEM images it can be found that in sample B, C, E and G, with higher carbon take-up rates, the carbon particles distributed in the fabrics also changed the structure of the fabrics as they filled some of the spaces between the fibres and connected nearby fibres together. In order to figure out if these changes in structure would further influence the performance of the pressure sensors, these four samples were picked out and made into pressure sensors for further tests (shown in Table 3).

Table 3. Samples used to create sensors

Sample number	Take-up rate (%)	Resistance(Ω)
B	70.6	1817
C	77.9	1623
E	84.3	1224
G	92.1	850

5.2.1 Electro-resistance tests:

There are several methods used to measure the electrical resistance. The mainly used methods are two-wire resistance measurement, four-wire resistance measurement and Wheatstone bridge circuit. Among them, two-wire measurement is the simplest (seen Figure 30 below), and the principle of it is based on the Ohms Law as:

$$R_{subject} + 2 \times R_{wire} = \frac{V_{voltmeter}}{L_{ammeter}} \quad (5\text{-}1)$$

In this equation, when the R_{wire} is small enough to be negligible, then $R_{subject}$ can be calculated as $V_{voltmeter}/I_{Ammeter}$. However, in the case that the subject is in a long distance away from the Ammeter and the Voltmeter, the R_{wire} is not negligible. The actual $R_{subject}$ is lower than the one calculated.

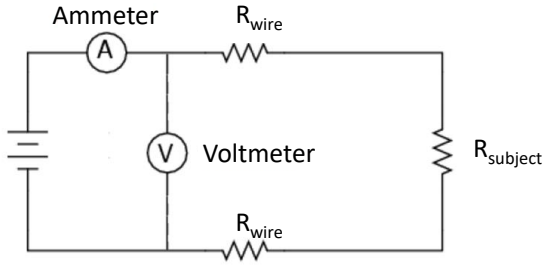

Figure 30. Two-wire resistance measurement

In order to avoid this error, the four-wire resistance measurement (shown in Figure 31) is used to take the R_{wire} into account. As the current on the voltmeter can be ignored,

$R_{subject}$ can be obtained from $V_{volmeter}/I_{Ammeter}$. The four-wire measurement setup helps to avoid the error caused by the extra electrical resistance of the long connection distance. It increases the accuracy of this research as there is a distance between the tensile tester and the computer. However, as the measurement range and accuracy of the four-wire setup are limited by the power supply, it is still not accurate enough to record the electrical resistance change of the textile sensors.

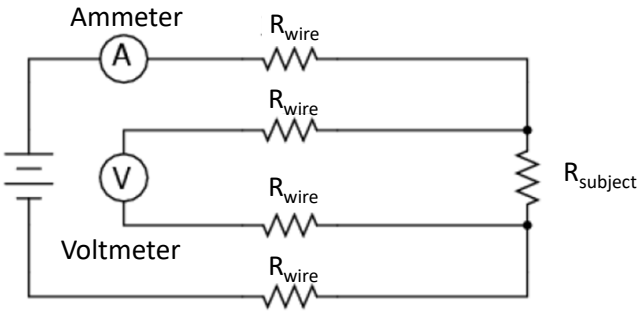

Figure 31. Four-wire resistance measurement

Based on all the requirements mentioned before, the Wheatstone bridge was finally chosen for electrical resistance measurement. The diagram of the Wheatstone bridge circuit is shown in Figure 32. In the diagram, the dotted lines are the circuit built into the data acquisition card.

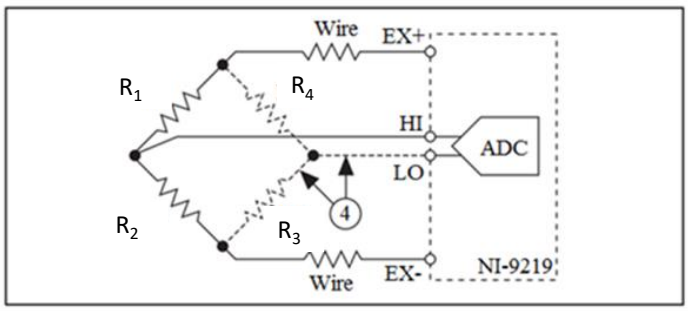

Figure 32. The Wheatstone bridge circuit diagram for the NI-9219

Generally speaking, when the bridge is fully balanced, which means there will be no output voltage, thus the voltage at HI and LO will be the same, thus no current will flow

through analogue-to-digital converter (ADC). The voltage at HI and LO can be measured based on the Ohm's law:

$$U_{HI} = U_{EX} \times \frac{R_1}{R_1 + R_2} \tag{5-2}$$

$$U_{HI} = U_{EX} \times \frac{R_4}{R_3 + R_4} \tag{5-3}$$

when the bridge is balanced,

$$U_{HI} = U_{EX} \tag{5-4}$$

$$\frac{R_1}{R_1 + R_2} = \frac{R_4}{R_3 + R_4} \tag{5-5}$$

The Wheatstone bridge can be further divided in to 3 types: full-bridge, half-bridge, and quarter-bridge. In full-bridge the resistance of all the resistors are different, in half-bridge two of the resistors are the same (they are usually R1 AND R2) while in quarter bridge three of the resistors are the same. The full-bridge is used in complicated cases where variable resistors exist and required to be measured. Half-bridge is usually used to accurately measure one single electrical resistance and the change of it. Quarter-bridge is used to measure the electrical resistance of an unknown but constant resistor.

In this research, the main focus is on the measuring the change in the electrical resistance so that half-bridge was used for measuring and recording of the electrical resistance in all types of tests involving electrical resistance. In order to measure the electrical resistance, the piezo-resistive sensor and a resistance box (*RR-box*) were connected into a half-bridge circuit as presented in Figure 33.

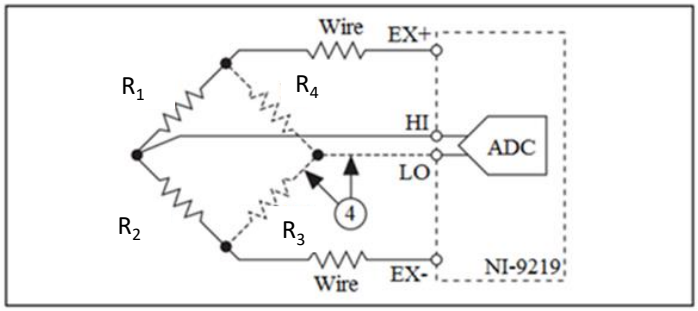

Figure 33. Half-bridge circuit diagram used to measure the resistance of the wearable sensor

The resistance box was used to balance the bridge the bridge. When the bridge was balanced and stable,

$$\frac{R_{sensor}}{R_{sensor} + R_{box}} = \frac{R_4}{R_4 + R_3} = \frac{1}{2} \tag{5-6}$$

which can be simplified as:

$$R_{sensor} = R_{box} \tag{5-7}$$

In dynamic conditions, the electrical resistances of the sensors change based on the variation of pressure applied on the sensor, which breaks the balance of the bridge. As the result, voltage difference appears between node HI and LO. Under this condition:

$$U_{HI-LO} = U_{HI-LO} \tag{5-8}$$

$$U_{HI-LO} = U_{EX} \times \frac{R_{sensor}}{R_{sensor} + R_{box}} - U_{EX} \times \frac{R4}{R3 + R4} \tag{5-9}$$

$$U_{HI-LO} = U_{EX} \times \frac{R_{sensor}}{R_{sensor} + R_{box}} - U_{EX} \times \frac{1}{2} \tag{5-10}$$

$$R_{sensor} = R_{box} \times \frac{1 - \frac{2 \times U_{HI-LO}}{U_{EX}}}{1 + \frac{2 \times U_{HI-LO}}{U_{EX}}} \tag{5-11}$$

With the help of NI-9219 data acquisition card (shown in Figure 34), the U_{HI-LO}/U_{EX}

during the tests can be measured and recorded.

Figure 34. NI-9219 data acquisition card

Several steps were taken to record a continuous resistance signal under dynamic conditions.

1) The bridge was balanced using the resistance box before starting the tests and the reading of the resistance box was noted.
2) The tests were carried out while U_{HI-LO}/U_{EX} results were recorded by NI-9219 data acquisition card.
3) Equation 5-11 was applied to calculator the dynamic electrical resistance of the sensor.

5.2.2 Electro-mechanical tests

1) Test conditioning

The test fabric materials were conditioned under the standard textile conditioning environment a 21 °C ± 2 °C and 65% ± 5% relative humidity for at least 24 hours based on ISO 139:2005.

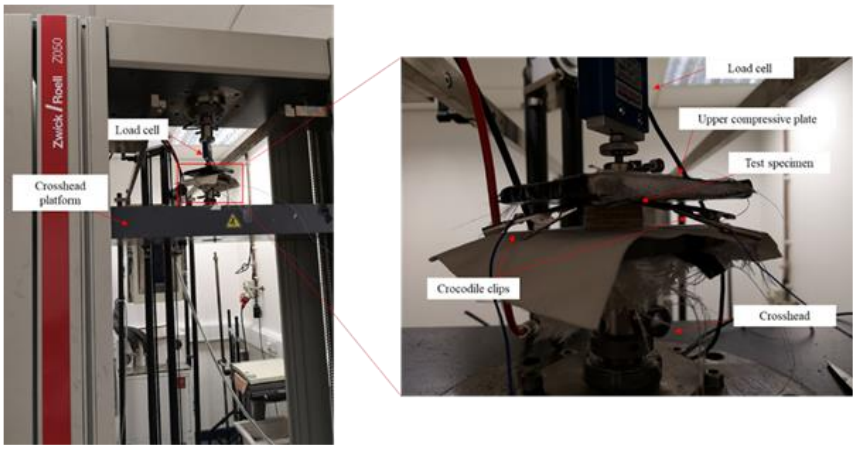

Figure 35. Zwick 050 tensile tester under compressive test settings

2) Quasi-static electro-mechanical compressive test

Quasi-static electro-mechanical test was carried out to investigate the piezo-resistivity of the textile based sensor while pressure was added on its surface. The results of this test would be used to analyze the working range of the sensor. The tests were performed with the help of Zwick 050 tensile tester (shown in Figure 35). The testing area of the sensor was set to be 40mm by 40mm with a deformation speed of 0.3 mm/min, till broken. During the testing process, the electrical resistance signals of the piezo-resistive nonwoven sensors were recorded and calculated by the NI-9219 data acquisition card and visualized in Signal Express 2012 software. For each samples five tests were done. With the help of this test, the relationship between resistance and pressure can be found.

3) Quasi-static electro-mechanical compressive test

Reproducibility of the fabric sensors were investigated using cyclic compressive load tests. By using Zwick 050 tensile tester, the sensor sample with the longest working range was compressed within their working range for 50 cycles, at a deformation speed of 0.3 mm/min for both loading and unloading cyclic. In order to analyze the reliability and stability of the best sample, a long term (400 cycles) test was done. The electrical

resistance was recorded at the same time using the same settings as the quasi-static electromechanical compressive test.

5.2.3 Scanning Electron Microscope (SEM) images

In order to figure out the distribution of carbon particles within the fabrics with different take-up rates, SEM images were taken. The SEM images were taken with the help of HITACHI 3000 and EVO 50. Images with magnifications of x100, x200, x500, x1000, x2000 and x5000 were taken.

5.3 Results and discussion

5.3.1 Compressive working range of the sensors

The working range of a compression sensor was determined by the change of its electro-resistance against the change of pressure force applied on it. If the resistance of the sensor does not change anymore with more pressure force applied, which means the sensors cannot react to any bigger force, then the sensor has reached its biggest working range. According to Figure 36, it can be found that fabric sample B had a biggest working range up to 60 g/cm^2. The working range decreased as the carbon take-up rates increased. In sample C, the biggest pressure can be sensed was decreased to 40g/cm^2, and in sample E it was further decreased to around 30 g/cm^2. While sample G with the biggest take-up rate, only had a working range up to around 16 g/cm^2.

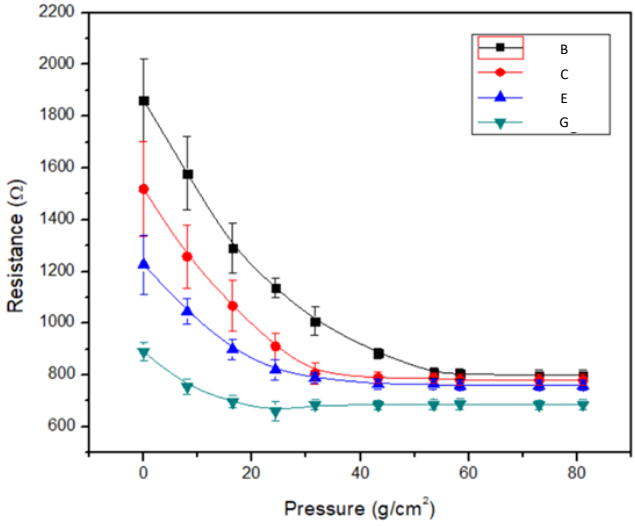

Figure 36. Resistance/pressure curve

Table 4. Working range and sensitivity of different samples

Sample	Take-up rate (%)	Working range (g/cm^2)	Sensitivity (KPa^{-1})
B	70.6	0-60	9.16
C	77.9	0-40	9.18
E	84.3	0-30	9.14
G	92.1	0-25	10.12

5.3.2 Sensitivity and reliability of the sensor

In order to test the repeatability and stability properties of the carbon-based textile pressure sensor, cyclic (loading and unloading) tests under its working range were done. As sample B showed the longest working range, it was picked out for this test. During the cyclic test, the sample was compressed to 8 N (within its working range).

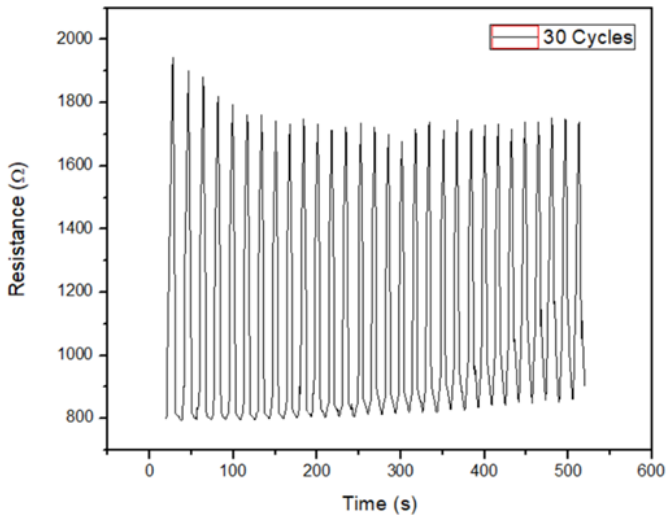

Figure 37. 30 cycles of the cyclic compressing test (sample B)

Figure 37 shows the change of resistance within 30 cycles of loading and unloading. It can be found that there is a decrease in the resistance at the very beginning (6 cycles). After that the resistance of the textile-based sensor is stable and shows a stable trend within 30 cycles. A possible reason for the decrease of resistance in the first 6 cycles is that the fabric needs to be conditioned under the test environment.

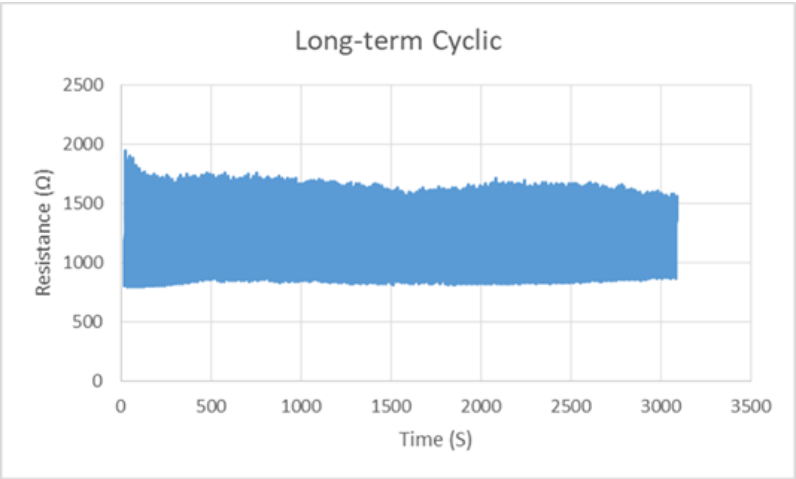

Figure 38. Long-term cyclic test of 400 cycles (sample B)

In order to figure out the stability of the sensor, a long-term stability test of 400 loading and unloading cyclic compressing test was done. It can be found from Figure 38 that

besides the first 6 cycles, the pressure sensor responded to the cyclic pressure of 400 cycles with a stable and inconspicuous electric variation. The amplitude exhibited no remarkable variation. When external pressure is applied, the gaps between fibres decreased. After the pressure is removed, the gaps recovered to the initial state gradually because of the reliability of textile-based sensor, which leads to the cyclic change of the electro-resistance during the test. The change of the electro-resistance of the sensor under pressure can be up to 55%. Based on these, it can be concluded that the ink used to coat the sensing fabric showed good sensitivity and high reliability.

Based on the stress/strain curve of the cyclic test, it can be found that the textile sensor showed a creep effect during the test. However, although the nonwoven fabric showed a big creep effect near the end of the test, the sensor can still detect the change of the pressure force applied to it, which indicate the sensor showed good reliability within 400 cycles.

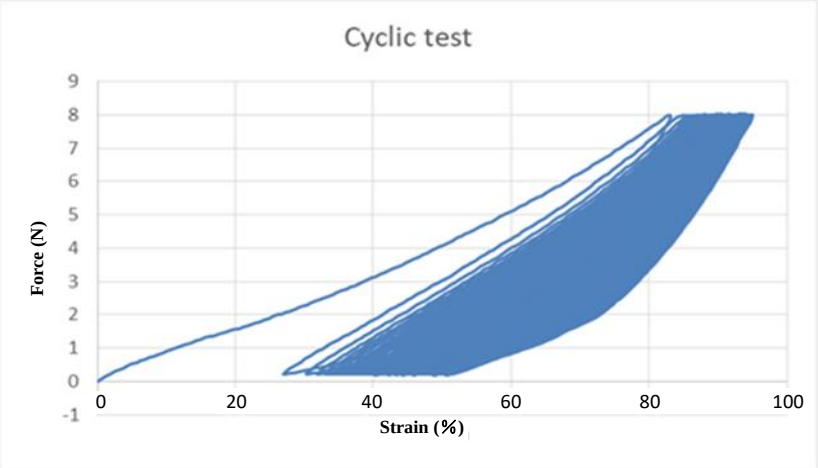

Figure 39. Stress and strain curve fur the 400 cycles

5.3.3 Effect of carbon particles distribution on the performance of the sensor

It could be found from this test that the working range of the sensors was related to the take-up rates of the samples. In order to figure out the relationship between them, SEM images of four samples were taken. Figure 40 shows the structure of the coated fabrics. The fibres within the fabric are coated with carbon particles which make them electro-conductive. From Figure 40-A, it can be found that the carbon coated fibres within the fabric create a connected network as the paths for the electrons to go through and make the fabric electro-conductive. While an outside pressure force is applied on the wearable sensor, the fabric deforms and the fibres on top and bottom become closer each other. When fibres within different planes get connected to each other, more electro-conductive paths are created which reduce the electro-conductivity of the sensor. That is why, with an increasing of the pressure force, the electro-resistance of the sensor decreases.

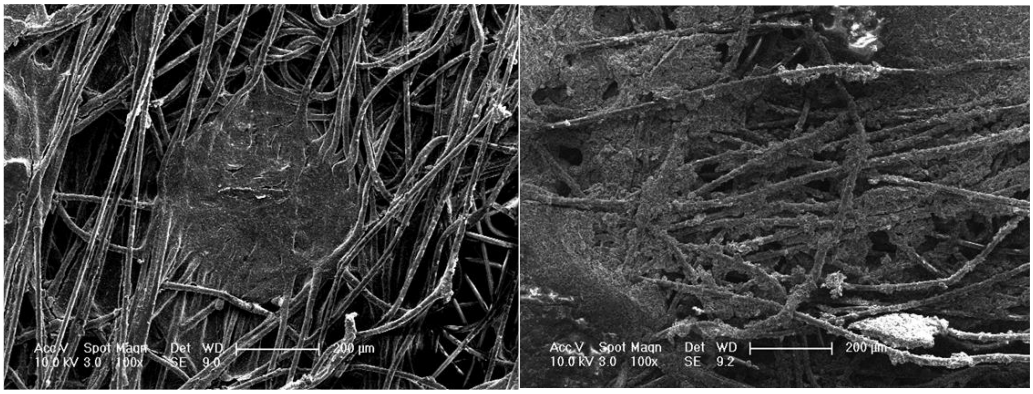

(A) Sample B (B)Sample C

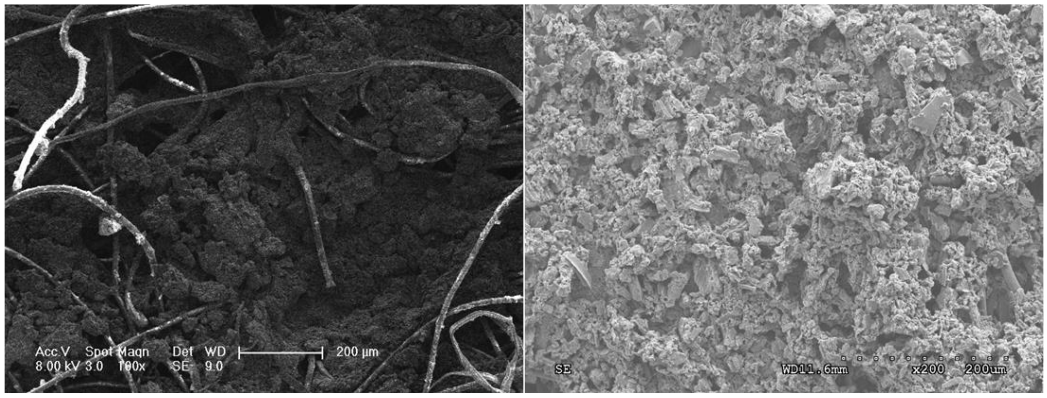

(C) Sample E (D) Sample G

Figure 40. SEM image of the four samples with magnification x100

Turning to samples with higher take-up rates, it can be found that more carbon particles are attached to the fabric. Some particles were on the surface of the fibres and others even filled the spaces between upper and lower (or nearby) fibres which connect them together. This leads to more electro-conductive paths created which makes the electro-resistance of them lower than that of fabrics with lower take-up rates.

As the spaces are already fully filled by carbon particles (which connects the fibres together), while outside compression force is applied to the sensor, there are less deformation space for the fibres. Because of that there are less connections between fibres can be made, which lead to a smaller changing range of the electro-resistance of the sensor. That is why sensors with a higher take-up rates show a lower working range

against outside pressure force.

5.3.4 Prevention of coffee ring effect

In order to get a further view of the distribution of carbon particles on the surface of the fibres, pictures of sample B with bigger magnifications were taken. The pictures with magnifications of x500, x1000, x2000 and x5000 are shown in Figure 41.

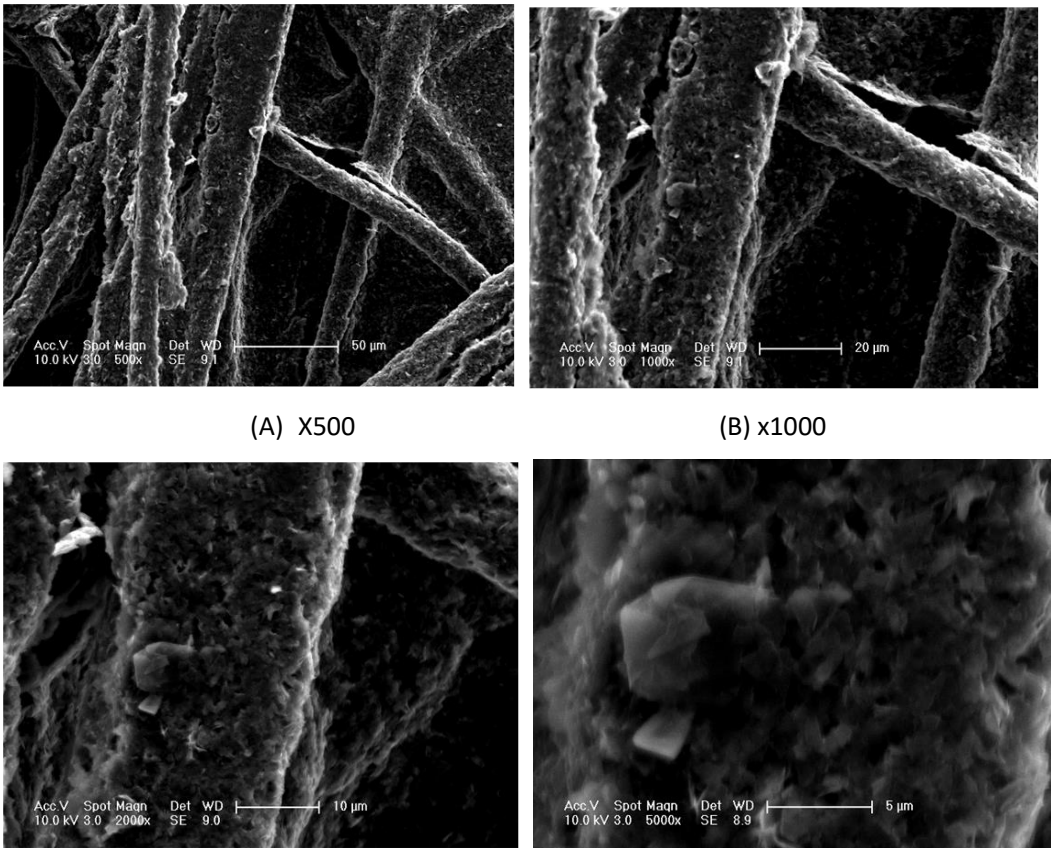

(A) X500 (B) x1000

(C) x2000 (D) x5000

Figure 41. SEM images of sample B with bigger magnifications. A) x500 B) x1000 C) x2000 D) x5000.

According the images in Figure 41, it can be found that the carbon particles are uniformly distributed on the surface on the fibres. With a magnification of x5000, no coffee ring effect was found. This indicates that the co-solvent used in this research worked and successfully avoid the coffee-ring effect.

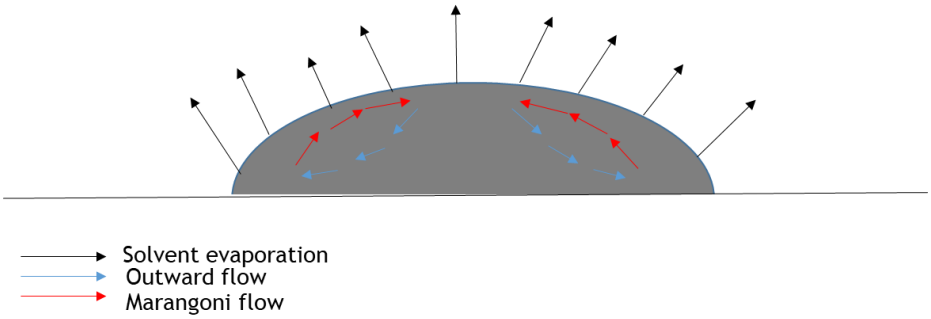

Figure 42. Working principle of Marangoni flow

Figure 42 showed the way of avoiding coffee ring effect into details, in this research the coffee ring effect was prevented with the help of the Marangoni flow theory. Coffee ring effect was usually caused during the drying process, usually the evaporation rate is the highest at the edge of the ink-substrate interface due to the highest surface area to volume ratio, because of that an outward flow was created from the centre of the ink to the edge to replenish the evaporated solvents. The co-solvent (Polyethylene glycol) added in this research have different properties against water (including viscosity, surface tension, density and so on). During the drying process, the differing solvent properties of water and polyethylene glycol can lead to variations in the solvent proportions across each ink droplets. As the results, surface tension, composition and temperature gradient are generated to drive an overall inward Marangoni flow to balance the outward flow and to avoid the coffee ring effect (Figure 42), this is why no coffee ring effect was seen according to the SEM images.

5.4 Summary

The performance of the ink was evaluated based on the wearable pressure sensors. It can be summarised that different carbon take-up rates have influence to the working range of the sensors. Carbon particles are uniformly distributed in sample A and no

coffee ring effect was found. According to the cyclic test within working range of sample B, the ink showed good conductivity, sensitivity and reliability over 400 cycles.

Chapter 6 Conclusions and further work

In this research, the components of electro-conductive carbon ink for wearable sensors were studied. According to the research in coffee ring effect, particle size, viscosity and surface tension, a type of water-based carbon ink free of coffee ring effect for fine nonwoven polyester fabrics was developed. In order to test the performance of the ink, it was used to coat nonwoven polyester fabrics to produce wearable pressure sensors.

6.1 Conclusions

Based on the work done in this research, conclusions can be summarised as follows.

1）After optimisation of the ink, the size of carbon particles within the ink are all smaller than 2μm. The viscosity of the ink was adapted and increased from 1mPa.s to 51 mPa.s under a shear rate of 500 s^{-1}. The surface tension of the ink was optimised to be 32 mN/m. With 0.1 mg/ml surfactant added to the ink, the carbon particles within the ink are stabilised. The ink is free from coffee ring effect.

2）Adding co-solvent with different surface tension against main solvent helped to avoid the coffee ring effect. Because of Marangoni effect, the differences in surface tension could cause a gradient and lead to an inward flow to balance the outward flow during drying process and prevent the coffee ring effect.

3）The take-up rates can affect the working range of the pressure sensor. It is found that if the take-up rate of the conductive fabric is too high (more than 90％). The fibres can be over-covered by carbon particles. The carbon particles filled the spaces between nearby fibres and make them connected together. This creates more conductive path and reduce the electro-resistance of the conductive fabric (around

850 Ω). However, higher take-up rates also reduce the deformation ability of the conductive fabric under pressure which further leads to a smaller working range (from 0 to less than 20g/cm^2). High take-up rates can be used in applications where only low electro-resistance is needed.

4）The ink coated sensor (with carbon take-up rate of 70.6%) in this research shows good conductivity, sensitivity and reliability under pressure of 60 g/cm^2 over 400 repeating cycles. With a concentration of 5 mg/ml, the ink successfully made fabrics conductive (with average electro-resistance of 1817Ω). The change of the electro-resistance of the sensor under pressure can be up to 55% which indicates a good sensitivity. The sensor showed a stable change in its resistance under a pressure of 60 g/cm^2 over 400 repeating cycles which approves that the ink has a good reliability.

6.2 Further work

In this research a water-based carbon ink for wearable sensor was produced. The ink showed good performance (conductivity, sensitivity and reliability) on wearable pressure sensor. However, there are still further researches needed to be done.

In this research, the ink was only designed for fine nonwoven polyester fabrics, if the ink could be used on other different types of fabrics should be further tested.

Washability is an important property for conductive inks. Further washability tests are needed. If the ink cannot achieve ideal washability, further researches are required.

References

[1] K.Chapman. High tech fabrics for smart garments. vol 2, 15–19, 2002.

[2] W.Deflin. Communication cloth: optical fibre fabric for a new flexible display. Advantex Proc, vol 3, 13–15, 2002.

[3] I. Hamedi, R. Mahiar and Forchheimer. Towards woven logic from organic electronic fibres. Nat. Mater, vol. 6, 357, 2007.

[4] S. Park, S. Mackenzie, K. Jayaraman, Framework for Personalized Mobile Information Processing (PMIP). In Proceedings of the 39th Design Automation Conference, pp. 10–14, 2002.

[5] A. Pantelopoulos and N. G. Bourbakis. A Survey on Wearable Sensor-Based Systems for Health Monitoring and Prognosis. IEEE Trans. Syst. Man, Cybern. Part C, vol. 40 (1), 1–12, 2010.

[6] N. Goncu-Berk, Gozde and Topcuoglu. A healthcare wearable for chronic pain management:Design of a smart glove for rheumatoid arthritis. Des. J, 20, 1978–1988, 2017.

[7] J. Meyer. Textile pressure sensor: Design, error modeling and evaluation. 155-160, 2008.

[8] F. Chiarugi et al. Measurement of heart rate and respiratory rate using a textile-based wearable device in heart failure patients. Comput. Cardiol, vol.3, 73-84, 2008.

[9] M. S. Sibinski, M. Jakubowska. Flexible temperature sensors on fibres. Sensors, vol.20, 48-56, 2010.

[10] A. M. Peltokangas, J. Verho. Night-time EKG and HRV monitoring with bed sheet integrated textile electrodes. IEEE Trans. Inf, Technol. Biomed, 255-258, 2012.

[11] O. A. and W. R. Kennon. Knitted strain sensors: Impact of design parameters on sensing properties. Sensors (Switzerland), vol.1, 53-59, 2014.

[12] A. Bonfiglio and D. De Rossi. Wearable monitoring systems, 271-279, 2011.

[13] D. R. McLaren, F. Joseph and C. Baguley. A review of e-textiles in neurological rehabilitation: How close are we? Rehabil, 740-750, 2016.

[14] L. E. Buechley et al. Fabric PCBs, electronic sequins, and socket buttons: Techniques for e-textile craft. Pers. Ubiquitous Comput, vol. 13, 133–150, 2009.

[15] T. Meoli, D. May-Plumlee. Interactive electronic textile development: A review of technologies. Technol. Manag, vol. 2, 1–12, 2012.

[16] N. Post, E.R.Orth, M.Russo, R.R.Gershenfeld. E-broidery: Design and fabrication of textile-based computing. IBM Syst, vol. 39, 840–860, 2000.

[17] G. Cottet, D. Grzyb, J. Kirstein, T. Tröster. Electrical characterization of textile transmission lines. IEEE Trans. Adv. Packag, vol. 26, 182–190, 2003.

[18] K. Suganuma. Printing Technoology. SpringerBriefs, 2014.

[19] M. Ukena. Plastisol vs. water-based ink for textile printing. Print. Environ. Technol, vol. 4, 8–11, 2005.

[20] Y.Wang, S.Ali, R.Gong and A.Fernando. A wearable piezo-resistive sensor for capturing cardiorespiratory signals. Sensors Actuators A Phys, 282, 215-229. 2018.

[21] Q. Cao, X. Geng, H. Wang, P. Wang, A. Liu, Y. Lan and Q. Peng. A review of current development of graphene mecanics. Crystals, vol. 8, 357, 2011.

[22] K.Suganuma. Printing technoogy. Springer, 175, 2014.
[23] T. A. Deegan and O.Bakajin. Capillary flow as the cause of the ring stains from dried liquid drops. Nature, vol. 389, 827–829, 1997.
[24] T. A. Deegan and O.Bakajin. Contact line deposites in an evaporating drop. Phys.Rev., vol. 62, 756–765, 2000.
[25] R. H. Hu. Marangoni effect reverses coffee-ring depositions. J.Phys.Chem.B, vol. 110, 7090–7094, 2006.
[26]R. H.Leach. The Printing Ink Manual. Springer, 257-259, 1993.
[27]D.N.Carvalho. Forty Centuries of Ink. Charleston: BiblioLife, 250-256, 2008.
[28]H. J. Goldschmidt and A. Streitberger. BASF handbook on basics of coating technology, 216-220, 2003.
[29] X. Jin, G. Hu, M. Zhang, Y. Hu, T. Albrow-Owen, C. T. Howe, T. Wu, Q. Wu, Z. Zheng. 102 fs pulse generation from a long-term stable, inkjet-printed black phosphorus-mode-locked fibre laser. ACS Nano, vol. 6, 2992–3006, 2012.
[30]R. J. Finn, M. Lotya, G. Cunningham, J. D. McCloskey, J. F. Donegan and J. N. Coleman. Inkjet deposition of liquid-exfoliated graphene and MoS2 nanosheets for printed device applications. Mater.Chem. C, vol. 2, 925–932, 2014.
[31]E. L. F. Withers, H. Yang, L. Britnell, A. P. Rooney et al. Engineering the Charge Transfer in all 2D Graphene-Nanoplatelets Heterostructure Photodetectors. Nano Lett, vol. 14, 3987–3992, 2014.
[32]A. G. Kelly, T. Hallam, C. Backes, A. Harvey, J. I. Godwin, J. Coelho, V. Nicolosi, J. Lauth, A. Kulkarni, S. Kinge and L. A. Siebbeles. All-printed thin-film transistors from networks of liquid-exfoliated nanosheets. Science, vol. 356, 69–73, 2017.
[33]V. S.-R. D. McManus, S. Vranic, F. Withers, C. M. Macucci, H. Yang, R. Sorrentino, K. Parvez, and K. Kostarelos. Applications of Printed 2D Materials. Nanotechnol, vol. 12, 343–350, 2017.
[34]I. T. Juntunen, H. Jussila, M. Ruoho, S. Liu, G. Hu, T. Albrow-Owen, R. C. T. Howe, T. Hasan, Z. Sun and Tittonen. Inkjet Printed Large-Area Flexible Few-Layer Graphene Thermoelectrics. Adv. Funct. Mater, vol. 10, 1002, 2018.
[35]T. Albrow-Owen, C. T. Richard, Z. Yang, X. Zhu, and R. I. Woodward. Black phosphorus ink formulation for inkjet printing of optoelectronics and photonics. Nat. Commu., vol. 8, 278, 2017.
[36]P. H. D. Dodoo-Arhin, R. C. T. Howe, G. Hu, Y. Zhang and T. H. A. Bello. Fully inkjet-printed two-dimensional material field-effect heterojunctions for wearable and textile electronics. Carbon N. Y., vol. 105, 33–41, 2016.
[37]T. H. H. Jussila, T. Albrow-Owen, H. Yang, G. Hu, S. Aksimsek, N. Granqvist, H. Lipsanen, R. C. T. Howe, Z. Sun. New Approach for Thickness Determination of Solution-Deposited Graphene Thin Films. ACS Omega, vol. 2, 1630, 2017.
[38]Z. A. Saynatjoki, L. Karvonen, H. Rostami, A. Autere, S. Mehravar, A. Lombardo, R. A. Norwood, T. Hasan, N. Peyghambarian, H. Lipsanen, K. Kieu, A. C. Ferrari and M. Polini. Ultra-strong nonlinear optical processes and trigonal warping in MoS2 layers. Nat. Commun, vol. 8, 893, 2017.
[39]Y. Xu, I. Hennig, D.Freyberg, A. J. Strudwick，M. G. Schwab. Multidimensional performance optimization of conducting polymer-based supercapacitor electrodes. J.

Power Sources, vol. 248, 483–488, 2014.
[40]A. W. C. Sriprachuabwong, C. Karuwan, J. D. Phokharatkul, T. Lomas, P. Sritongkham and A.Tuantranont. Highly selective phosphorescent nanoprobes for sensing and bioimaging of homocysteine and cysteine. Mater. Chem, vol. 22, 5478, 2012.
[41]F. G. Karagiannidis, S. A. Hodge, L. Lombardi, S. V. M. N. Decorde, S. Milana, I. Goykhman, Y. Su, N. N. Johnstone, R. K. Leary, P. A. Midgley, and F. T. and A. C. Ferrari. Microfluidization of Graphite and Formulation of Graphene-Based Conductive Inks. ACS Nano, vol. 11, 2742–2755, 2017.
[42]B. K. Park, D. Kim, S. Jeong and J. Moon. Direct writing of copper conductive patterns by ink-jet printing. ScienceDirect, vol. 515, 7706–7711, 2007.
[43] D. Li, D. Sutton and A. Burgess. Conductive copper and nickel lines via reactive inkjet printing. Mater. Chem., vol. 10, 10, 2009.
[44]C. j. Jyun and E. B. Secor. All-printed,foldable organic thin-film transistors on glassine paper. Adv.Mater, vol. 27, 7058–7064, 2015.
[45] W.Zhang, X. Li and H. Li. Graphene-based counter electrode for dye-sensitized solar cells. Carbon N. Y., vol. 49, 5382–5388, 2011.
[46]Q.Zhang, F.Zhang and C.Zhou. 3D printing of graphene aerogels. Smart Mater. Struct., vol. 12, 1702–1708, 2016.
[47]E. S. R.Bell and S.Eslava. Printing and three dimensions with graphene. Adv.Mater, vol. 27, 157–161, 2015.
[48]E. A. Tretyakov and V.A.Lukashin. Synthesis of functional nanocomposites based on solid-phase nanoreactors. Russ Chem, vol. 73, 899–921, 2004.
[49]H. A. Kimura K. Fine particles. Synthesis, characterization, and mechanisms of growth. Surf Sci Ser, vol. 92, 513–550, 2000.
[50]S. H. Mafune, J. Kohno, Y.Takeda and T.Kondow. Formation and size control of silver nanoparticles by laser ablation in aqueous solution. J Phys Chem B, vol. 104, 9111–9117, 2000.
[51]K. A. Magdassi and M.Grouchko. Colloidal dispersion of metal nanoparticles: formation and functional properties. Structure and functional properties of colloidal systems, 339–365,2010.
[52]O. P. Dearden, P.J.Smith, N.Reis and B.Derby. A low curing temperature silver ink for use in ink-jet printing and subsequent production of conductive tracks. Macromol Rapid Commun, vol. 26, 315–318, 2005.
[53]C.J.Curtis, T.Rivkin and A.Miedaner. Metallizations by directwrite inkjet printing. Mat Res Soc Symp Proc, vol. 730, 79–84, 2002.
[54]S. J. Rozenberg, E.Bresler, S.P.Speakman and C.Jeynes. Patterned low temperature copper-rich deposits using inkjet printing. Appl Phys Lett, vol. 81, 5249–5251, 2002.
[55]S. J. Rozenberg. Synthesis and spectroscopic studies of novel diketonate copper(I) compounds and solid state structure of tetravinylsilane tetrakis copper(I) 1,1,1,5,5,5-hexafluoroacetylacetonate (TVST[Cu]hfac). Organometallics, vol. 20, 4001–4005, 2001.
[56]G. W. Rockenberger and F. Zurcher. Aluminum inks and methods of making the same, methods for depositing aluminum inks, and films by printing and/or depositing

an aluminum ink. Springer, 228-237, 2010.
[57]V. P. Campbell, R. K. Kalia and A. Nakano A. Dynamics of oxidation of aluminum nanoclusters using variable charge moleculardynamics simulations on parallel computers. Phys Rev Lett, vol. 82, 4866–4869, 1999.
[58]H. K. Foley and C. E. Johnson. Inhibition of oxide formation on aluminum nanoparticles by transition metal coating. Chem Mater, vol. 17, 4086–4091, 2005.
[59]J.J.Chun. Review on preparation technology and application of activated carbon. Chem. Ind., vol. 1, 235–240, 2017.
[60]G. T. C. Mattmann and F. Clemens. Sensor for measuring strain in textile. Sensors,vol 20, 168-169, 2008.
[61]L. Capineri. Resistive sensors with smart textiles for wearable technology: From fabrication processes to integration with electronics. Procedia Eng, vol. 23, 176, 2014.
[62]P. L. Guo, Y. Huang, X. Cai and C. Liu. Capacitive wearable tactile sensor based on smart textile substrate with carbon black /silicone rubber composite dielectric. Meas. Sci. Technol, vol 10, 98, 2016.
[63]Y. C.Wei, S. X. Mei and W. Bo. Developing process of carbon nanotubes. Mater. Guid., vol. 26, 424, 2007.
[64]T. Yamada et al. A stretchable carbon nanotube strain sensor for human-motion detection. Nat. Nanotechnol, vol. 3, 52, 2011.
[65]M. W. Han, B. Kim and J. Li. A carbon nanotube based ammonia sensor on cotton textile. Appl. Phys.lett, vol.49, 166-167, 2013.
[66] M. R. E. Devaux, C. Aubry and C. Campagne. PLA/carbon nanotubes multifilament yarns for relative humidity Textile sensor. J. Eng. Fibre. Fabr, vol. 2, 160-162, 2011.
[67]J. Foroughi et al. Knitted Carbon-Nanotube-Sheath/Spandex-Core Elastomeric Yarns for Artificial Muscles and Strain Sensing. ACS Nano, vol. 6, 74-76, 2016.
[68]C.C.Xin. Direct electrochemistry of horseradish peroxidase on carbon nanotube electrode. Acta Chim. Sin., vol. 44, 83-88, 2014.
[69]H. C. Xiu, L.J.Hong. Structure, properties and applications of carbon nanotubes. J. Shenzhen Univ. (Science Technol. Ed.), vol. 1, 763, 2013.
[70]J. N. Hughes, J Marguerite, A.Damian and Coleman,. Generalizing solubility parameter theory to apply to one-and two-dimensional solutes and to incorporate dipolar interactions. J. Appl. Polym. Sci., vol. 127, 4483–4491, 2013.
[71]J. N. Varrla, P. Eswaraiah, R. Keith, H. Claudia, S. Andrew, J. McCauley and Coleman. Turbulence-assisted shear exfoliation of graphene using household detergent and a kitchen blender. Nanoscale, vol. 6, 1819-1820, 2014.
[72]E. Bush, Karen, P. Dantas, G. Davies, J. Eisenstein, B. Huovinen, P. Jacoby, G. Kishony, R. Kreiswirth and B. Kutter. Tackling antibiotic resistance. Nat. Rev. Microbiol., vol. 9, 894, 2011.
[73]P. Kossyrev. Carbon black supercapacitors employing thin electrodes. J. Power Sources, vol. 201, 347–352, 2012.
[74]J. Zhu and H. Huang. Preparation of graphene and its application in electrochemistry. Chem.ANA, vol. 3, 768, 2011.
[75]L.Song and P.Wu. Research progress of carbon based two-dimensional crystal

materials. J. China Univ. Sci. Technol., vol. 5, 254-256, 2014.
[76]Z. Yang et al. Graphene Textile Strain Sensor with Negative Resistance Variation for Human Motion Detection. ACS Nano, vol. 18, 28-30, 2018.
[77]B. Xun, W. Meng, J. Pan, X. Lei Luo, D. Cheng, G. Cai and Jin.Wang. Conductive Cotton Fabrics for Motion Sensing and Heating Applications. Polymer (Guildf., vol. 10, 568, 2018.
[78]C. S. Boland et al. Sensitive, high-strain, high-rate bodily motion sensors based on graphene-rubber composites. ACS Nano, vol. 25, 262-263, 2014.
[79]R. K. Layek and A. K. Nandi. A review on synthesis and properties of polymer functionalized graphene. Polymerer, vol. 224, 53-57, 2013.
[80]B. Yun, W. G. Hong, W. J. Kim and Y. Jun. A novel method for applying reduced graphene oxide directly to electronic textiles from yarns to fabrics. Adv. Mater, vol. 24, 223-224, 2013.
[81]Y. Jiang, X.Wang, Q. Wang, X. Li, X. Zhang, J. Golberg and D.Bando. Recent progress on fabrications and applications of boron nitride nanomaterials: a review. J. Mater. Sci.& Technol., vol. 31, 589–598, 2015.
[82]Z. Liu, Lei. Feng and Y. Shen. Structural and electronic properties of h-BN. Phys. Rev. B, vol. 68, 102-104, 2003.
[83]T. Mir, P. Audiffred and M. Heine. An atlas of two-dimensional materials. Chem. Soc. Rev., vol. 43, 6537–6554, 2014.
[84]T. Li, Q. Chen, L. Gadinski, R. Matthew, Z. Zhang, Gu. Li, H. Iagodkine, E. Haque, A. Chen and L. Jackson. Flexible high-temperature dielectric materials from polymer nanocomposites. Nature, vol. 523, 576, 2015.
[85]S. Kim, Wun-gwi and Nair. Membranes from nanoporous 1D and 2D materials: A review of opportunities, developments, and challenges. Chem. Eng. Sci., vol. 104, 908–924, 2013.
[86]S. C. Kou, L. Chen and C.Smith. Phosphorene: fabrication, properties, and applications. J. Phys. Chem. Lett., vol. 6, 2794–2805, 2015.
[87]Z.Zolek-Tryznowska. Printing on Polymers. Elsevier, vol. 9, 11-12, 2016.
[88]K. Barnes, A. Hutton and J. Walters. An Introduction to Rheology. 291-293, 1989.
[89]L. A.Gudkova. The relation between rheological properties of printing inks and their behaviour in the printing process. Nauch, vol. 11, 219–245, 1959.
[90]T. Hartford. Rheological Measurement of Printing Ink Vehicles at Low Shear Conditions. Am. Inkmak., vol. 72, 42–51, 1994.
[91]K. Dalwadi, H. Canet, C. Roye and N. Hedman. Rheology: an important tool in ink development. Am. Lab., vol. 37, 18–23, 2005.
[92]N. Coquel, F. Godlewski and E. Seguin. Relaxation of fluid systems. Math. Model. Methods Appl. Sci., vol. 22, 124-125, 2012.
[93]D.V Boger. An introduction to rheology. Non-Newtonian Fluid Mech, vol. 32, 331–332, 1989.
[94]H. Green. Rheological properties of paints, varnishes, lacquers, and printing inks. J. Sci., vol. 2, 93–98, 1947.
[95]Z.Z.Tryznowska. Printing on polymers. Elsevier, 175-177, 2016.
[96]G. Batchelor. An Introduction to Fluid Dynamics. Cambridge University Press,

294-296, 1970.
[97]J. E. Buchdahl and R.Thimm. The relationship between the rheological properties and working properties of printing inks. J. Appl. Phys., vol. 16, 344–350, 1945.
[98]B. J. Kirby. Micro and nanoscale fluid mechanics: transport in microfluidic devices. Cambridge university press, 1-11, 2010.
[99]D. Kundu, K. Pijush, C. Ira and M. Dowling. Fluid Mechanics 4th. Elsevier, 23, 2008.
[100]O. Oittinen, P. Pirkko and I. Perila. Rheological Properties of printing inks. Suom. Kemistil., vol. 45, 95, 1972.
[101]A. L. Tropea and C. Yarin. Springer handbook of experimental fluid mechanics. Springer Science & Business Media, 121-133, 2007.
[102]O. Oittinen, Pirkko and Perila. Flow curve and tack behaviour and the packing of paper. Suom. Kemistil., vol. 45(3), 95, 1972.
[103]T. Watanabe, Koichiro and Amari. Rheological properties of coatings during drying processes. J. Appl. Polym. Sci., vol. 32 (2), 3435--3443, 1986.
[104]A. Mishra, P. Mukherjee, S. Nayak and S. Kumar. A brief review on viscosity of nanofluids. Int. nano Lett., vol. 4 (4), 109--120, 2014.
[105]J. F. Steffe. Rheological methods in food process engineering. Freeman press, 81, 1996.
[106]E. C. Bingham. An investigation of the laws of plastic flow. US Government Printing Office, 141, 1917.
[107]J. Black, Lin Long and M. Guthrie Electrochemical sensors. US5658444A, 1997.
[108]P. Ciesielski and A. Samori. Graphene via sonication assisted liquid-phase exfoliation. Chem. Soc. Rev., vol. 23, 187-189, 2014.
[109]M. C. Green, A. Alexander and A. Hersam. Solution Phase Production of Graphene with Controlled Thickness via Density Differentiation. Nano Lett, vol. 10, 2009.
[110]S. J. Hadson, C. E. Gabriella, B. de-Melloab, Lily Smith, J. Rowley-Nealebc and Jonas Grubera. Surfactant-exfoliated 2D molybdenum disulphide (2D-MoS2): the role of surfactant upon the hydrogen evolution reaction. RSC Adv, vol. 7, pp. 36208–36213, 2017.
[111]T. J. Gregory, W.J. Longmore and M.A. Moxley. Surfactant chemical composition and biophysical activity in acute respiratory distress syndrome. J. Clin. Invest., vol. 88, 1978–1981, 1992.
[112]V. P. Torchilin. Structure and design of polymeric surfactant-based drug delivery systems. J. Controlled release, vol. 73, 137–172, 2001.
[113]J. C. A. Ciesielski, S. Haar, M. El Gemayel, H. Yang, G. L. G. Melinte, M. Gobbi, E. Orgiu, M. V. Nardi, P. S. V. Palermo, N. Koch and O. Ersen. Harnessing the Liquid-Phase Exfoliation of Graphene Using Aliphatic Compounds: A Supramolecular Approach. Angew. Chemie Int. Ed., 843-857, 2014.
[114]Y. T. Liang and M. C. Hersam. Highly Concentrated Graphene Solutions via Polymer Enhanced Solvent Exfoliation and Iterative Solvent Exchange. Am. Chem. Soc, vol. 132, 17661–17663, 2010.
[115]Y. Baeg, P. Kang-Jun and Caironi Mario. Toward printed integrated circuits based

on unipolar or ambipolar polymer semiconductors. Adv. Mater., vol. 25, 4210–4244, 2013.
[116]Z. Ping. Fabric detection and performance design. China Text. Press, vol. 16, 134-137, 2018.
[117]C. X .Chen. Textile quality standard and inspection. 48-53, 2018.
[118]C. S. A.Thomasson. Development of Cotton Fibre Quality Sensor, 82, 2009.
[119]C. R.Jun. Design of Cotton Sliver Detecting Sensor. Intrument Tech. Sens., vol. 6, 52-53, 2009.
[120]M.Corp. Cotton moisture sensor. https://www.moisttech.com/applications/textile-moisture/cotton-moisture/, 2020.
[121]Y. Zhang. Modern textile testing technology, ChinaTextile&Apparel Press. 68-74, 2017.
[122]Y. Lee, J. Kim, H. Wang, S. Jeong. Highly stretchable and sensitive strain sensors based on single-walled carbon nanotube-coated nylon textile. Korean J. Chem. Eng., vol. 36, 800–806, 2019.
[123]T. K. Toprakci. Textile sensors. Handb. smart Text., 357–379, 2015.
[124]X. Z. Zhang, Hongqiang Li, Xuejun Lai, Tianyuan Gao and Jian Yang. Thiolated Graphene Polyester Fabric-Based Multilayer Piezoresistive Pressure Sensors for Detecting Human Motion. ACS Appl. Mater. Interfaces, vol. 10, 1021, 2018.
[125]P. Y. Lisa LaFleur. Medical Biosensors. Biomater. Sens., 122-128, 2013.
[126]M. S. Kim. Wearable body sensor network for health care applications. Smart Text. their Appl., 51-53, 2016.
[127]S. M. Tian, M. Pan. Sensor Materials, Technologies and Applications. Compr. Mater. Process., vol. 14, 28, 2014.
[128]C. B. Mecnika, K. Scheulen, C. F. Anderson, M. Hörr. Joining technologies for electronic textiles. Electron. Text. Smart Fabr. Wearable Technol., vol. 43, 63-64, 2015.
[129]Y.D.Cai, Modern weaving technology. 22, 2008.
[130]T. G. V. Mecnika, M. Hoerr, I. Krievins and S. Jockenhoevel. Technical Embroidery for Smart Textiles. Mater. Sci. Text. Cloth. Technol,vol. 22, 134-135, 2015.
[131]S. J. P. Bosowski, M. Hoerr, V. Mecnika, T. Gries. Design and manufacture of textile-based sensors. Electron. Text. Smart Fabr. Wearable Technol., vol. 23, 104, 2015.
[132]W.L.Li. Study on the final performance of synthetic Satin yarn for woven fabrics. China Text. Press, vol. 30, 22, 2019.
[133]X.M.Gu. Performance evaluation and test of textile products. China Text. Press, vol. 33, 170-173, 2019.
[134]M. Stoppa and A. Chiolerio. Wearable electronics and smart textiles: A critical review. Sensors (Switzerland), 843-857, 2014.
[135]M. Rothmaier and F. Clemens. Textile pressure sensor made of flexible plastic optical fibres. EMPA Act., vol. 12, 56-59, 2008.
[136]R. Paradiso and M. Pacelli. Textile electrodes and integrated smart textile for reliable biomonitoring. Annual International Conference of the IEEE Engineering in Medicine and Biology Society, 2011.
[137]O. Chetelat. New biosensors and wearables for cardiorespiratory telemonitoring.

3rd IEEE EMBS International Conference on Biomedical and Health Informatics. 2016.
[138]J. Li and B. Xu. Novel highly sensitive and wearable pressure sensors from conductive three-dimensional fabric structures. Smart Mater. Struct, vol. 27, 112-113, 2015.
[139]R. M. Pacelli, G. Loriga and N. Taccini. Sensing fabrics for monitoring physiological and biomechanical variables: E-textile solutions. 3rd IEEE-EMBS International Summer School and Symposium on Medical Devices and Biosensors. 2006.
[140]T. Garen and K. Klopp. Methoden zur Verfahrensbewertung. Oberflächentechnologien für Textilien, 2007.
[141]F.Pan. Modern wool spinning technology. China Text. Press, vol. 26, 188-192, 2017.
[142]X. H. Zhang and C. Y. Zhu. Principle and application of modern weaving. China Text. Press, 319-320, 2017.
[143]X.M.Wang. Textile process design. China Text. Press, 506-516, 2016.
[144]J.Y.Tian. Functional textiles.China Text. Press, 118-126, 2015.
[145]Y.J.Liu. Handbook of spunbond and melt blown nonwovens. China Text. Press, 78-81, 2014.
[146]D. Satas. Web processing and converting technology and equipment. Van Nostrand Reinhold Company, 1984.
[147]Guzman G, Dahmani B and Puetz J. Transparent conducting sol-gel ATO coatings for display applications by an improved dip coating technique. Thin Solid Films, vol. 502, 281–285, 2006.
[148]G. E. Cohen. Modern coating and drying technology. Wiley-VCH, 1992.
[149]A. N. Ratcliff and Lee P a. Work function control of hole-selective polymer/ITO anode contacts: an electrochemical doping study. J Mater Chem, vol. 20, 2672, 2010.
[150]Wang D, Li F and Zhao J. Fabrication of Graphene/Polyaniline Composite Paper via In Situ Anodic Electropolymerization for High-Performance Flexible Electrode. ACS Nano, vol. 3, 1745–1752, 2009.
[151]C. M. Zhu, L. M. Li and J. H. Wang. Three-dimensional highly conductive silver nanowires sponges based on cotton-templated porous structures for stretchable conductors. RSC Adv, vol. 7, 51–57, 2017.
[152]C. David, N. David and Y. Katz. Electro-conductive fabrics based on dip coating of cotton in poly(3-hexylthiophene). Polym Adv Technol, vol. 28, 583–589, 2017.
[153]Y. J. Liu and S. Hu. A facile way of fabricating flexible and conductive cotton fabric. J Mater Chem C, vol. 4, 1320–1325, 2016.
[154]F. R. Kaynak. Methods of coating textiles with soluble conducting polymers. Res J Text Appar, vol. 15, 107–113, 2011.
[155]O. Irwin and R. Roberson. Conductive polymer-coated threads as electrical interconnects in e-textiles. Fibres Polym, vol. 12, 904–910, 2011.
[156]J. W. Koenig and J. Shenk. How automatic metrology systems help to increase product quality while saving production costs and time. ICE, 141-48, 2015.
[157]P. Tompson. “Dark field technologies, high speed, high resolution coating inspection. ICE, 2015.

[158]H. M.Singh. Inkjet printing-process and iys applications. Adv. Mater., vol. 22, 673–685, 2016.
[159]I. M. Hutchings, G. Graham and D. Martin. Inkjet technology for digital fabrication, 22, 2010.
[160]P. G.Korvink. Inkjet-based micromanufacturing. 78-81, 2012.
[161]P.Calvert. Inkjet printing for materials and devices. Chem Mater, vol. 13, 3299–3305, 2001.
[162]S. E.Tekin and P.J.Smith. Inkjet printing as a depositon and patterning tool for polymers and inorganic particles. Soft Matter, vol. 4, 703, 2008.
[163]S. C. Duineceld. Inkjet printing of polymers :state of the art and future developments. Adv. Mater, vol. 16, 203–213, 2004.
[164]Öhlund T. Coated Surfaces for Inkjet-Printed Conductors. 2012.
[165]T. Carey et al. Fully inkjet-printed two-dimensional material field-effect heterojunctions for wearable and textile electronics. Nat. Commun., vol. 8, 198-201, 2017.
[166]Z. S. F.Torrisi, T.Hasan, W.Wu. Inkjet printed graphene electronics. ACS Nano, vol. 6, 2992–3006, 2012.
[167]N. Tasaltin, D. Sanli,A.Jonáš. Preparation and characterization of superhydrophobic surfaces based on hexamethyldisilazane-modified nanoporous alumina. Nanoscale Res Lett, vol. 6, 487, 2011.
[168]G. M. Chinga-Carrasco G and Kuznetsova N. Bleached and unbleached MFC nanobarriers: properties and hydrophobisation with hexamethyldisilazane. 231-236, 2018.
[169]Ö. R. Chinga-Carrasco G and Tobjörk D. Inkjet-Printed silver nanoparticles on nano-Engineered cellulose films for electrically conducting structures and organic transistors: Concept and challenges. J Nanoparticle Res, vol. 14, 157-160, 2012.
[170]M. A. Andersson H and Rusu A. System of nano-silver inkjet printed memory cards and PC card reader and programmer. Microelectron. J, vol. 42, 20–27, 2011.
[171]B.Derby. Inkjet printing of functional and structural materials: fluid property requirements feature stability, and resolution," Mater. (Basel）, vol. 40, 395–414, 2010.
[172]S. F. Rosu and R.A.Shanks. Shear rheology and thermal properties of linear and branched poly blends. Polymer (Guildf), vol. 40, 5891–5898, 1999.
[173]C. B. Kang and W.H.Lee. Recent advances in organic transistor printing process. ACS Appel. Mater, vol. 5, 2302–2315, 2013.
[174]S. E. S.Scherp. Silkscreen Printing Machine. US4267773, 1981.
[175]F. A. Owczarek. A study of the off-contact screen printing process. Hybrids Manuf.Technol, vol. 13, 358–367, 1990.
[176]D. He. Modelling and computer simulation of behaviour of solder paste in stencil printing for surface mout assembly. PhD thesis, 1998.
[177]P. N. Kapur, E. D. Dolden. Predicting the behaviour of screen printing. IEEE Trans.Compon.Package, vol. 3, 508–515, 2013.
[178]A. C. Karuwan and A. Wisitsoraat. Screen-printed graphene-based electrochemical sensors for microfluidic device. Anal.Methods, vol. 9, 3689–3695,

2017.
[179]H. F. K.Arapov and E.Rubingh. Conductive screen printing inks by gelation of graphene dispersions. ADV.Funct.Mater, vol. 26, 586–593, 2016.
[180]K. mulle, Y.Xu and M. G. Schwab.Screen-printable thin film supercapacitor device utilizing graphene/polyaniline inks. Adv.Engery Mater, vol. 3, 1035–1040, 2013.
[181]C. J. Rowley-Neale and G.C.Smith. Mass-producible 2D-MoS2-impregnated screen-printed electrodes. ACS Appel. Mater, vol. 9, 22539–22548, 2017.
[182]K. A. M. Abdelkader and C. Valles. Ultraflexible and robust graphene supercapacitors printed on textiles for wearble electronics applications. 2D Mater, vol. 4, 35016, 2017.
[183]K. M. Joseph. Screen-printable electronic ink of ultrathin boron nitride nanosheets. ACS Omega, vol. 1, 1220–1228, 2016.
[184]H.Lievens. Wide web coating of complex materials. Surf.Coat.Techno, vol. 76, 744–753, 1995.
[185]K.I.Bardin. Gravure printing method. US4003311, 1977.
[186]V. L. M. Lahti. Gravure-offset-printing technique for the fabrication of solid films. APPL.Surf.Sci., vol. 142, 367–370, 1999.
[187]D. L. Nguyen and C.LEE. An investigation of the ink-transfer mechanism during the printing phase of high-solution roll-to-roll gravure printing. IEEE Trans. Adv. Packag., vol. 5, 1516–1524, 2015.
[188]D. D.Nguyen, J.Lee and C.H.Kim. An approach for controlling printed lin-width in high resolution roll-to-roll gravure printing. J.Micromech.Microeng, vol. 23, 95-100, 2013.
[189]H.Kipphan. Handbook of Print Media. Berlin: Springer, 2001.
[190]Printwiki. Anilox roller. http://printwiki.org/Anilox_Roller, 2018.
[191]J.A.Martens. Flexographic printing plate process. US5172072.
[192]R.N.Fan. Laser ablatable photosensitive elements utilized to make flexographic printing plates. US5719009, 1990.
[193]M. C. Van, L. C.Schubert. Innovations in 3D printing:a 3D overview from optics to organs. BR.J.Ophthalmol, vol. 98, 159–161, 2014.
[194]T. M. Baker and D. T. Gethin. Flexographic printing of graphene nanoplatlet ink to replace platimun as counter electrode catalyst in flexible dye sensitised solar cell. Mater.Res.Innov, vol. 18, 86–90, 2014.
[195]M. E. Jakus, E. B. Secor. Three-dimensional printing of high-content graphene scaggolds for electronic and bionedical applications. ACS Nano, vol. 9, 4636–4648, 2015.
[196]W. Y. Xiao, Q.Zhang and S.Xu. Gravure printing of hybrid MoS20eGO interdigitated electrodes for flexible microsupercapacitors. Appl Phys Lett, vol. 107, 139-142, 2015.
[197]T.Smith. Flexographic inks. Pigm.Resin Technol, vol. 15, 11–12, 1986.
[198]S. R. Holler, F. James, Skoog, Douglas and A. Crouch. Principles of Instrumental Analysis (6th ed.), 843-855, 2007.
[199]R. S. C. Manbachi and A. Cobbold. Development and Application of Piezoelectric Materials for Ultrasound Generation and Detection. Ultrasound, vol. 19, 187–196, 2011.

[200]G. Gautschi. Piezoelectric Sensorics: Force, Strain, Pressure, Acceleration and Acoustic Emission Sensors. Mater. Amplifiers, vol. 10, 54, 2002.
[201] Y. Jiang, H. Hamada and S. Shiono. A PVDF-based flexible cardiorespiratory sensor with independently optimized sensitivity to heartbeat and respiration. Procedia Eng, vol. 5, 1466–1469, 2010.
[202]Kevin Magniez, Andrew Krajewski, Martin Neuenhofer and Richard Helmer. Effect of drawing on the molecular orientation and polymorphism of melt-spun polyvinylidene fluoride fibres: Toward the development of piezoelectric force sensors. Appl. Polym. Sci., vol. 129, 2699–2706, 2013.
[203]M. G. Nihtianov. Application challenges of capacitive sensors with floating targets. IEEE AFRICON Conf, 13–15, 2012.
[204]L. K. Baxter. Capacitive Sensors. 155-157, 1996.
[205]N. A. Gao and V. Arcos V. Piezoelectric vs. Capacitive Based Force Sensing in 177 Capacitive Touch Panels. IEEE Access, vol. 4, pp. 1374–1375, 2016.
[206]G. Radosavljević, L. Živanov and W. Smetana. A wireless embedded resonant pressure sensor fabricated in the standard LTCC technology. IEEE Sens J, vol. 9, 1956–1962, 2009.
[207]M. Sergio. A Textile Based Capacitive Pressure Sensor. IEEE Conference, 2002.
[208]C. González-Sánchez, J. Fraile and J. Pérez-Turiel. Capacitive Sensing for Non-Invasive Breathing and Heart Monitoring in Non-Restrained, Non-Sedated Laboratory Mice. Sensors, vol. 16, 52, 2016.
[209]S. H. Park et al. Development of A Textile Capacitive Proximity Sensor and Gait Monitoring System for Smart Healthcare. Mob. Wirel. Heal., vol. 42, 76, 2018.
[210]C. M. Bakhoum EG et al. High-sensitivity inductive pressure sensor. IEEE Trans Instrum Meas, vol. 60, 2960–2966, 2011.
[211]W. Thomson. On the Electro-Dynamic Qualities of Metals:--Effects of Magnetization on the Electric Conductivity of Nickel and of Iron. Proc. R. Soc, vol. 8, 546–550, 1856.
[212]W. A. Brantley. Calculated elastic constants for stress problems associated with semiconductor devices. J. Appl. Phys., vol. 44, 534–535, 1973.
[213]W. R. K. O. Atalay, A. Tuncay and M. D. Husain. Comparative study of the weft-knitted strain sensors. J. Ind. Text, vol. 46, 1212–1240, 2017.
[214]S. M. S. Salibindla, B. Ripoche and D. T. H. Lai. Characterization of a new flexible pressure sensor for body sensor networks. IEEE Eighth Int. Conf. Intell. Sensors, Sens. Networks Inf. Process., 27–31, 2013.
[215]F. A. Hamdani and Potluri P. Thermo-mechanical behavior of textile heating fabric based on silver coated polymeric yarn. Mater. (Basel）, vol. 6, 1072–1089, 2013.
[216]C. L. I. Baldoli, M. Maselli and F. Cecchi. Development and characterization of a multilayer matrix textile sensor for interface pressure measurements. Smart Mater. Struct., vol. 26, 91-97, 2017.
[217]R. E. Bicking. Fundamentals of Pressure Sensor Technology. 663-668, 1998.
[218]G. Lee rt al. Next Generation Pressure Sensors In Surface Micromachining Technology. 13th International Conference on Solid-State Sensors, Actuators and Microsystems, 35–36, 2005..

[219]G. Sworn. Xanthan gum. Handbook of hydrocolloids, Elsevier, 186–203, 2009.
[220]M. Montero, P. Solas and T.Prez-Mateos. Pressure-induced gel properties of fish mince with ionic and non-ionic gums added. Food Hydrocoll, vol. 15, 185–194, 2001.
[221]M. Chaplin. Water structure and behavior: guar gum. London South Bank Univ., 11, 2006.
[222]D. Koley and A. J. Bard. Triton X-100 concentration effects on membrane permeability of a single HeLa cell by scanning electrochemical microscopy (SECM). Proc. Natl. Acad. Sci. USA, vol. 107, 16783–16784, 2010.
[223]F. C. Krebs. Fabrication and processing of polymer colar cells: a review of printing and coating trchniques. Energy master, vol. 93, 394–412, 2009.
[224]A.Eich, Visco Handbook. 538-544, 2015.
[225]Y. Wei, R. Torah and K. Yang. Screen printing of a capacitive cantilever-based motion sensor on fabric using a novel sacrificial layer process for smart fabric applications. Meas Sci Technol, vol. 25, 956–959, 2013.
[226] AFM and Piezoresponsive Materials. Http://www. nanophys .kth. se/ nanophys/facilities/nfl/afm/icon/brukerContent/PiezoResponse_NSV/Piezoelectric%20Effect.htm.
[227]D. M. A.Eastwood. The dietary effects of xanthan gum in man. Food Addit.Contam, vol. 4, 17–26, 1987.
[228]V. O. Sheftel. Indirect food additives and polymers: migration and toxicology. 223-227, 2000.

Appendix

MATLAB code for 3D graph for viscosity and surface tension

```
clear all
figure
x=xlsread('Book_XYZ.xlsx',1);%area
y=xlsread('Book_XYZ.xlsx',2);%pressure
z=xlsread('Book_XYZ.xlsx',3);%resistance
% surf(x,y,z/1000)
Xq=0:1:3;
Yq=0:1:3;
[Xq,Yq] = meshgrid(Xq,Yq);
zq=interp2(x,y,z,Xq,Yq,'cubic');
surf(Xq,Yq,zq/1000)
shading interp
hold on
```